

CMS-TOP-13-004

CERN-EP/2016-044
2016/08/30

Measurement of the $t\bar{t}$ production cross section in the $e\mu$ channel in proton-proton collisions at $\sqrt{s} = 7$ and 8 TeV

The CMS Collaboration*

Abstract

The inclusive cross section for top quark pair production is measured in proton-proton collisions at $\sqrt{s} = 7$ and 8 TeV, corresponding to 5.0 and 19.7 fb^{-1} , respectively, with the CMS experiment at the LHC. The cross sections are measured in the electron-muon channel using a binned likelihood fit to multi-differential final state distributions related to identified b quark jets and other jets in the event. The measured cross section values are $173.6 \pm 2.1 \text{ (stat)}^{+4.5}_{-4.0} \text{ (syst)} \pm 3.8 \text{ (lumi)} \text{ pb}$ at $\sqrt{s} = 7$ TeV, and $244.9 \pm 1.4 \text{ (stat)}^{+6.3}_{-5.5} \text{ (syst)} \pm 6.4 \text{ (lumi)} \text{ pb}$ at $\sqrt{s} = 8$ TeV, in good agreement with QCD calculations at next-to-next-to-leading-order accuracy. The ratio of the cross sections measured at 7 and 8 TeV is determined, as well as cross sections in the fiducial regions defined by the acceptance requirements on the two charged leptons in the final state. The cross section results are used to determine the top quark pole mass via the dependence of the theoretically predicted cross section on the mass, giving a best result of $173.8^{+1.7}_{-1.8} \text{ GeV}$. The data at $\sqrt{s} = 8$ TeV are also used to set limits, for two neutralino mass values, on the pair production of supersymmetric partners of the top quark with masses close to the top quark mass.

Published in the Journal of High Energy Physics as doi:10.1007/JHEP08(2016)029.

1 Introduction

The study of top quark pair ($t\bar{t}$) production in proton-proton (pp) collisions at the CERN LHC provides an important test of the standard model (SM). The total production cross section, $\sigma_{t\bar{t}}$, can be accurately predicted by quantum chromodynamics (QCD) calculations at next-to-next-to-leading order (NNLO). A measurement of $\sigma_{t\bar{t}}$ can thus provide constraints on essential ingredients in the calculation, such as the top quark mass, the proton parton distribution functions (PDFs), and the strong coupling α_s . Furthermore, deviations from these predictions can be an indication of physics beyond the SM. For example, in supersymmetric (SUSY) models, $t\bar{t}$ pairs may appear as decay products of heavier new particles, increasing the $t\bar{t}$ yields.

Studies of the $t\bar{t}$ production cross section, as well as dedicated searches for deviations from the SM predictions, have been performed in recent years by the ATLAS and CMS collaborations using a variety of production and decay channels [1–22]. So far, all results are consistent with the SM.

This paper presents a new measurement of $\sigma_{t\bar{t}}$ in pp collisions at centre-of-mass energies of 7 and 8 TeV. The measurement is performed in the $e\mu$ channel, where each W boson from the top quark decays into a charged lepton and a neutrino. Compared to the previous CMS analyses in the dilepton channel at 7 TeV [8] and 8 TeV [1], the new measurement is performed using the complete CMS data samples recorded in the years 2011 and 2012, with integrated luminosities of 5.0 and 19.7 fb^{-1} at $\sqrt{s} = 7$ and 8 TeV, respectively. The restriction to the $e\mu$ channel provides a pure $t\bar{t}$ event sample owing to the negligible contamination from Z/γ^* processes with same-flavoured leptons in the final state. The event selection is based on the kinematic properties of the leptons. An improved cross section extraction method is used, performing a template fit of the signal and background contributions to multi-differential binned distributions related to the multiplicity of b quark jets (referred to as b jets in the following) and the multiplicity and transverse momenta of other jets in the event. The results obtained with this method (referred to as the “reference method” in the following) are cross-checked with an analysis performed using an event counting method.

The cross section is first determined in a fiducial (“visible”) range, $\sigma_{t\bar{t}}^{\text{vis}}$, defined by requirements on the transverse momentum and pseudorapidity of the electron and muon. The results are then extrapolated to obtain the cross section in the full phase space, $\sigma_{t\bar{t}}$, with an additional assessment of the extrapolation uncertainties. The ratio of the cross sections at the two centre-of-mass energies is also presented. The measurements of $\sigma_{t\bar{t}}$ at 7 and 8 TeV are used to determine, together with the NNLO prediction [23], the top quark pole mass. Following a previous CMS analysis [24], the mass is determined via the dependence of the theoretically predicted cross section on the top quark mass.

The data are also used to constrain the cross section of pair production of the lightest supersymmetric partner of the top quark, the top squark, in the context of SUSY models with R -parity conservation [25]. The study focuses on models predicting the decay of top squarks into a top quark and a neutralino, $\tilde{t} \rightarrow t\tilde{\chi}_1^0$, and the three-body decay, $\tilde{t} \rightarrow bW\tilde{\chi}_1^0$, with the neutralino assumed to be the lightest supersymmetric particle (LSP) [26]. The pair production and the subsequent decays of the top squarks can lead to a final state that is very similar to the SM $t\bar{t}$ events. The search is performed with the 8 TeV data, looking for an excess of the observed event yields of $t\bar{t}$ events with respect to the SM predictions. Exclusion limits are set with 95% confidence level (CL) for the SUSY signal strength as a function of the top squark mass for two neutralino mass hypotheses. Previous measurements setting exclusion limits in a similar regime can be found in [14, 27].

This paper is structured as follows. Section 2 contains a brief description of the CMS detector, followed by details of the event simulation and theoretical calculations for the $t\bar{t}$ cross section are given in Section 3. The event selection and the definitions of the visible and total cross sections are given in Sections 4 and 5, respectively. The methods used to measure the cross section are explained in Section 6 and the systematic uncertainties are described in Section 7. The measured $t\bar{t}$ production cross sections are reported in Section 8, with the extraction of the top quark mass presented in Section 9. The search for SUSY is described in Section 10 and a summary is provided in Section 11.

2 The CMS detector

The central feature of the CMS apparatus is a superconducting solenoid of 6 m internal diameter, providing a magnetic field of 3.8 T. Within the solenoid volume are a silicon pixel and strip tracker, a lead tungstate crystal electromagnetic calorimeter (ECAL), and a brass and scintillator hadron calorimeter (HCAL), each composed of a barrel and two endcap sections. Extensive forward calorimetry complements the coverage provided by the barrel and endcap detectors. Muons are measured in gas-ionisation detectors embedded in the steel flux-return yoke outside the solenoid. A more detailed description of the CMS detector, together with a definition of the coordinate system used and the relevant kinematic variables, can be found in Ref. [28].

The particle-flow (PF) [29, 30] event algorithm reconstructs and identifies each individual particle with an optimised combination of information from the various elements of the CMS detector. The energy of photons is directly obtained from the ECAL measurement. The energy of electrons is determined from a combination of the electron momentum at the primary interaction vertex as determined by the tracker, the energy of the corresponding ECAL cluster, and the energy sum of all bremsstrahlung photons spatially compatible with originating from the electron track. The energy of muons is obtained from the curvature of the corresponding track. The energy of charged hadrons is determined from a combination of their momentum measured in the tracker and the matching ECAL and HCAL energy deposits, corrected for zero-suppression effects and for the response function of the calorimeters to hadronic showers. Finally, the energy of neutral hadrons is obtained from the corresponding corrected ECAL and HCAL energy.

3 Event simulation and theoretical calculations

Experimental effects, related to the event reconstruction and choice of selection criteria, together with the detector resolution, are modelled using Monte Carlo (MC) event generators interfaced with a detailed detector simulation. Unless specified, the same generators and parton shower models are used for the samples at 7 and 8 TeV.

The $t\bar{t}$ sample is simulated using the MADGRAPH event generator (v. 5.1.5.11) [31], which implements the relevant matrix elements at tree level with up to three additional partons. The MADSPIN [32] package is used to incorporate spin correlation effects. The value of the top quark mass is fixed to 172.5 GeV and the proton structure is described by the CTEQ6L1 [33] PDF set. The generated events are subsequently processed with PYTHIA (v. 6.426) [34] for parton showering and hadronisation, and the MLM prescription [35] is used for matching of matrix-element jets to parton showers. Decays of τ leptons are handled with TAUOLA (v. 2.75) [36]. An additional $t\bar{t}$ signal sample, which is used to determine specific model uncertainties of the measurement, is obtained with the next-to-leading-order (NLO) generator POWHEG (v. 1.0 r1380) [37] and also interfaced with PYTHIA. In POWHEG, the value of the top quark

mass is also set to 172.5 GeV, and the CT10 [38] PDF set is used to describe the proton structure. The PYTHIA Z2* tune, derived from the Z1 tune [39], is used to characterise the underlying event in the $t\bar{t}$ samples at 7 and 8 TeV. The Z1 tune uses the CTEQ5L PDF set, whereas Z2* adopts CTEQ6L. The propagation of the generated particles through the CMS detector and the modelling of the detector response is performed using GEANT4 (v. 9.4) [40].

Only $t\bar{t}$ pair decays into $e^\pm \mu^\mp + X$ in the final state are considered signal, including intermediate leptonic τ decays. The remaining $t\bar{t}$ decay modes are considered background processes and referred to as “ $t\bar{t}$ bkg.”.

The other SM background samples are simulated with MADGRAPH (without the MADSPIN package), POWHEG, or PYTHIA, depending on the process. The main background contributions originate from the production of W and Z/γ^* bosons with additional jets (referred to in the following as W+jets and Drell–Yan (DY), respectively), single top quark tW channel, diboson (WW, WZ, and ZZ, referred to as VV in the following), $t\bar{t}$ production in association with a Z, W, or γ boson (referred to as $t\bar{t}V$ in the following), and QCD multijet events. The W+jets, DY, and $t\bar{t}V$ samples are simulated with MADGRAPH with up to two additional partons in the final state. The POWHEG [41, 42] generator is used for simulating single top quark production, while PYTHIA is used to simulate diboson and QCD multijet events. Parton showering and hadronisation are also simulated with PYTHIA in all the background samples. The PYTHIA Z2* tune is used to characterise the underlying event in the background samples at $\sqrt{s} = 8$ TeV, while the Z2 tune [43] is used at $\sqrt{s} = 7$ TeV.

The simulated samples are normalised according to their expected total cross sections for integrated luminosities of $5.0(19.7)\text{ fb}^{-1}$ for $\sqrt{s} = 7(8)$ TeV. The expected cross sections are obtained from NNLO calculations for W+jets [44] and DY [45] processes, NLO+next-to-next-to-leading-log (NNLL) calculations for top quark tW or $\bar{t}W$ channel [46], NLO calculations for VV [47], $t\bar{t}+W$ [48], and $t\bar{t}+Z$ [49] processes, and leading-order (LO) calculations for QCD multijet events [34].

A number of additional pp simulated hadronic interactions (pileup) are added to each simulated event to reproduce the multiple interactions in each bunch crossing in the data taking. The pileup events are generated using PYTHIA. Scale factors (SFs) described in Section 4 are applied when needed to improve the description of the data by the simulation.

Calculations of the $\sigma_{t\bar{t}}$ at full NNLO accuracy in perturbative QCD, including the resummation of NNLL soft-gluon terms [50], are used to normalise the $t\bar{t}$ simulated samples and to extract the top quark pole mass. Assuming a top quark mass of 172.5 GeV, the predicted cross sections are:

$$\begin{aligned}\sigma_{t\bar{t}} &= 177.3^{+4.7}_{-6.0}(\text{scale}) \pm 9.0(\text{PDF}+\alpha_s) \text{ pb}, & \text{at } \sqrt{s} = 7 \text{ TeV and} \\ \sigma_{t\bar{t}} &= 252.9^{+6.4}_{-8.6}(\text{scale}) \pm 11.7(\text{PDF}+\alpha_s) \text{ pb}, & \text{at } \sqrt{s} = 8 \text{ TeV.}\end{aligned}$$

The first uncertainty is an estimate of the effect of missing higher-order corrections and is determined by independent variations of the factorisation and renormalisation scales, μ_F and μ_R , by factors of two, up and down from their default values (the top quark mass). The second uncertainty is associated with variations in α_s and the PDF, following the PDF4LHC prescription with the MSTW2008 68% CL NNLO, CT10 NNLO, and NNPDF2.3 5f FFN PDF sets (as detailed in Refs. [51, 52] and references therein, as well as in Refs. [53–55]). These values were calculated using the TOP++2.0 program [50]. The ratio of the cross sections at 7 and 8 TeV computed with NNPDF2.3, $R_{t\bar{t}}^{\text{NNLO}} = \sigma_{t\bar{t}}(8 \text{ TeV}) / \sigma_{t\bar{t}}(7 \text{ TeV})$, is 1.437 ± 0.001 (scale) ± 0.006 (PDF) ± 0.001 (α_s) [56].

4 Event selection

At trigger level, events are required to have one electron and one muon. For the 8 TeV data set one of the two leptons is required to have $p_T > 17 \text{ GeV}$ and the other $p_T > 8 \text{ GeV}$. For the 7 TeV data set both leptons are required to have $p_T > 10 \text{ GeV}$ or to fulfil the same criterion as for the 8 TeV data set. The $e\mu$ trigger efficiency is measured in data with a method based on triggers that are uncorrelated with those used in the analysis [1, 57]. In particular, the triggers require jets or missing transverse energy, which is defined as the magnitude of the projection, on the plane perpendicular to the beam direction, of the vector sum of the momenta of all reconstructed particles in an event. The trigger efficiency for events containing an $e\mu$ pair passing all selection criteria is approximately 96% at 7 TeV and 93% at 8 TeV. Using the $e\mu$ trigger efficiency measured in data, the corresponding efficiencies in the simulation are corrected by η -dependent SFs, which have an average value of 0.99 at 7 TeV and 0.97 at 8 TeV.

An interaction vertex [58] is required within 24 cm of the detector centre along the beam line direction, and within 2 cm of the beam line in the transverse plane. Among all such vertices, the primary vertex of an event is identified as the one with the largest value of the scalar sum of the p_T^2 of the associated tracks.

Leptons are required to have $p_T > 20 \text{ GeV}$ and $|\eta| < 2.4$. The lepton-candidate tracks are required to originate from the primary vertex.

Lepton candidates are required to be isolated from other PF candidates in the event. For each electron [59] or muon [60] candidate, a cone with $\Delta R = 0.3$ or 0.4, respectively, is constructed around the track direction at the primary vertex. Here ΔR is defined as $\Delta R = \sqrt{(\Delta\eta)^2 + (\Delta\phi)^2}$, where $\Delta\eta$ and $\Delta\phi$ are the differences in pseudorapidity and azimuthal angle (in radians) between any PF candidate and the lepton track direction. The scalar sum of the p_T of all PF candidates contained within the cone is calculated, excluding the contribution from the lepton candidate itself. All charged PF candidates not associated with the chosen primary vertex are assumed to arise from pileup events, and are excluded from the calculation of the p_T deposited in the cone. The neutral component is also corrected for pileup effects. The relative isolation discriminant, I_{rel} , is defined as the ratio of this sum to the p_T of the lepton candidate. An electron candidate is selected if $I_{\text{rel}} < 0.10$; the corresponding requirement for muons is $I_{\text{rel}} < 0.12$.

The efficiency of the lepton selection is measured using a “tag-and-probe” method in dilepton events enriched with Z boson candidates [8, 61]. The measured values for the combined identification and isolation efficiencies are typically 80% for electrons and 90% for muons. The lepton identification efficiencies in simulation are corrected to the measured values in data by p_T and η dependent SFs, which have values in the range 0.97–0.99. From all events that contain oppositely charged lepton pairs, events are selected if the lepton pair with the largest value of the scalar sum of the p_T corresponds to an $e\mu$ pair. Candidate events with $e\mu$ invariant masses $m_{e\mu} < 20 \text{ GeV}$ are removed to reduce the contamination from QCD multijet processes. This selection is referred to as “ $e\mu$ selection”.

Jets are reconstructed using the anti- k_T clustering algorithm [62] with a distance parameter $R = 0.5$. The algorithm uses the PF candidates as input objects. To minimise the impact of pileup, charged particle candidates not associated with the primary vertex are excluded. The jet energy is corrected for pileup in a manner similar to the correction of the total energy inside the lepton isolation cone. Additional jet energy corrections are also applied as a function of the jet p_T and η [63]. Jets are selected if they have $p_T > 30 \text{ GeV}$ and $|\eta| < 2.4$ and the angular distance between them and the selected leptons satisfies $\Delta R(\text{jet}, \text{lepton}) > 0.5$.

As the $t\bar{t}$ events are expected to contain mainly jets from the hadronisation of b quarks, re-

quiring the presence of b jets can reduce background from events without b quarks. Jets are identified as b jets (b-tagged) using the combined secondary vertex algorithm [64]. The discriminator threshold chosen for the reference method to extract the cross section corresponds to an identification efficiency for b jets of about 50% and a misidentification (mistag) probability of about 10% for c quark jets and 0.1% for light-flavour jets (u, d, s, and gluons). A looser discriminator threshold is chosen for the event counting method such that the efficiency is about 70% for jets originating from b quarks and 20% for c quark jets, while the probability of mistagging for jets originating from light flavours is around 1% [64]. For the reference method there are no constraints on the number of jets and b-tagged jets in the event.

Figures 1 and 2 show for the 7 and 8 TeV data and simulations, respectively, the p_T and η distributions of the highest (leading) and second-highest (subleading) p_T lepton from the selected $e\mu$ pair, after the $e\mu$ selection is applied. The data are compared to the expected distributions for the $t\bar{t}$ signal and individual backgrounds, which are derived from MC simulated samples. The contributions from QCD multijet, W+jets, and $t\bar{t}$ background processes arise from events where at least one jet is incorrectly reconstructed as a lepton or a lepton that does not originate from a prompt W or Z boson decay fulfils the selection criteria. These contributions are referred to as “non W/Z” background.

In general, the sum of the estimated contributions provides an adequate description of the data, within uncertainties. However, as observed previously [57], the simulation is seen to have a somewhat harder p_T spectrum than measured. The impact on the measurement is accounted for by including an additional modelling uncertainty.

Figure 3 shows the number of b-tagged jets in events passing the $e\mu$ selection at 7 and 8 TeV. It should be noted that the size of the uncertainties in Figs. 1–3 does not reflect those in the final measurements, which are constrained by the likelihood fit described in Section 6.1. Good agreement is observed between data and the sum of the expected yields.

5 Cross section definitions

The $t\bar{t}$ production cross sections are first measured in a fiducial range, defined within the kinematic acceptance of the $t\bar{t}$ decay particles that are reconstructable in the detector. This avoids the need for extrapolating the cross sections into the unmeasured kinematic phase space of these particles. In this analysis the fiducial range is defined by the p_T and η requirements on the electron and muon in the final state. The visible cross section, $\sigma_{t\bar{t}}^{\text{vis}}$, is defined for events containing an oppositely charged $e\mu$ pair from the decay chain $t \rightarrow Wb \rightarrow \ell\nu b$ (including $W \rightarrow \tau\nu \rightarrow \ell\nu\nu\nu$) and with both leptons satisfying $p_T > 20 \text{ GeV}$ and $|\eta| < 2.4$. This visible cross section is then extrapolated to obtain the cross section for $t\bar{t}$ production at parton level in the full phase space using the formula

$$\sigma_{t\bar{t}} = \frac{\sigma_{t\bar{t}}^{\text{vis}}}{A_{e\mu}}. \quad (1)$$

Here, $A_{e\mu}$ denotes the acceptance defined as the fraction of all $t\bar{t}$ events fulfilling the above selection criteria for the visible cross section. The acceptance is determined from the simulated $t\bar{t}$ signal sample, and includes the leptonic branching fraction of the W bosons of 10.86% [65].

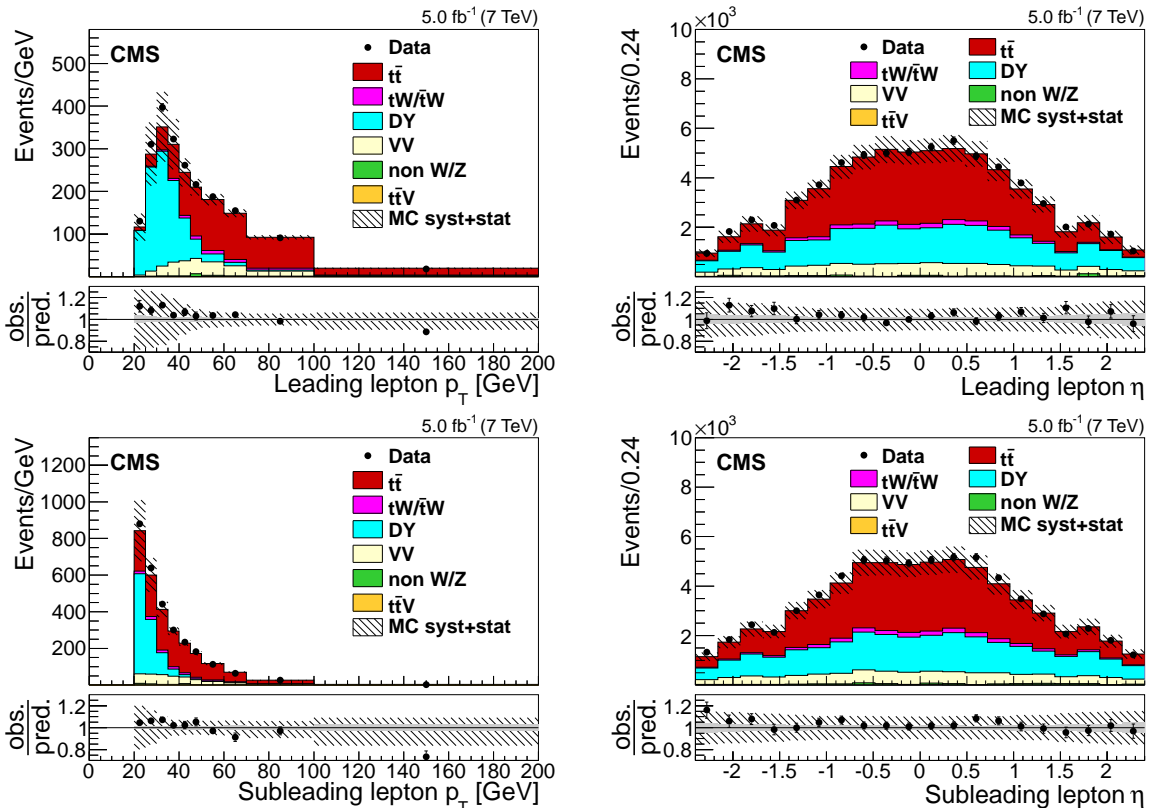


Figure 1: Distributions of p_T (left) and η (right) of the leading (top) and subleading (bottom) leptons, after the $e\mu$ selection, for the 7 TeV data. The last bin of the p_T distributions includes the overflow events. The hatched bands correspond to the total uncertainty in the sum of the predicted yields. The ratios of data to the sum of the predicted yields are shown at the bottom of each plot. Here, an additional solid gray band represents the contribution from the statistical uncertainty in the MC simulation. The contributing systematic uncertainties are discussed in Section 7.

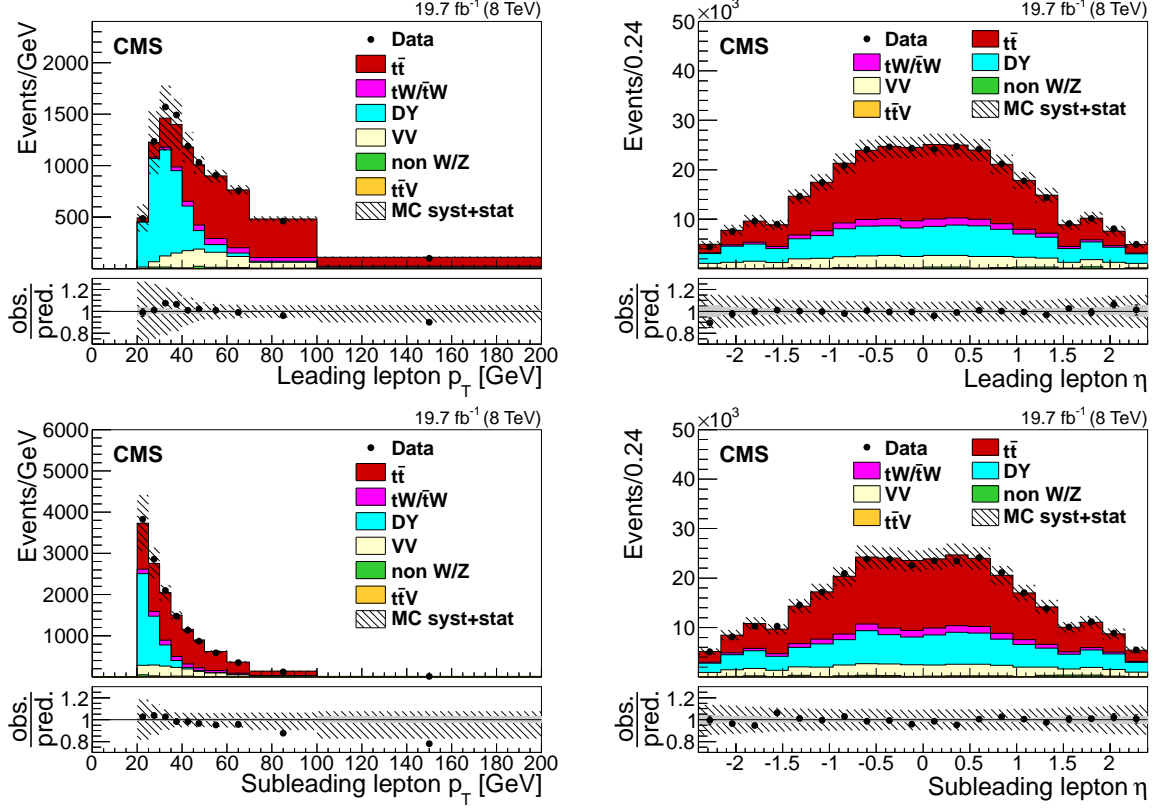


Figure 2: Distributions of p_T (left) and η (right) of the leading (top) and subleading (bottom) leptons, after the $e\mu$ selection, for the 8 TeV data. The last bin of the p_T distributions includes the overflow events. The hatched bands correspond to the total uncertainty in the sum of the predicted yields. The ratios of data to the sum of the predicted yields are shown at the bottom of each plot. Here, an additional solid grey band represents the contribution from the statistical uncertainty in the MC simulation. The contributing systematic uncertainties are discussed in Section 7.

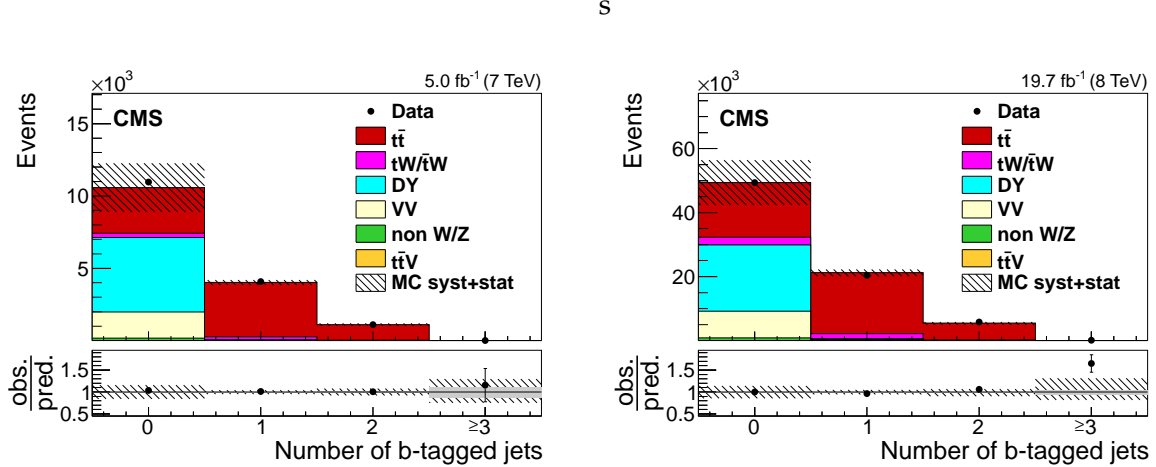


Figure 3: Number of b-tagged jets after the $e\mu$ selection for 7 TeV (left) and 8 TeV (right). The hatched bands correspond to the total uncertainty in the sum of the predicted yields. The ratios of data to the sum of the predicted yields are shown at the bottom of each plot. Here, an additional solid grey band represents the contribution from the statistical uncertainty in the MC simulation. The contributing systematic uncertainties are discussed in Section 7.

6 Analysis methods for the measurement of the cross section

Two methods are used to measure the $t\bar{t}$ production cross section. The reference method is a binned likelihood fit to multi-differential final state distributions, performed in categories of number of additional and b-tagged jets, as described in Section 6.1. In addition, an analysis is performed using an event counting technique, as explained in Section 6.2.

6.1 Binned likelihood fit

An extended binned likelihood fit is applied to determine $\sigma_{t\bar{t}}^{\text{vis}}$. The expected signal and background distributions are modelled in the fit by template histograms constructed from the simulated samples. The free parameters in the fit are $\sigma_{t\bar{t}}^{\text{vis}}$, the background normalisation parameters $\vec{\omega} = (\omega_1, \omega_2, \dots, \omega_K)$ for the K sources of backgrounds, and the M nuisance parameters $\vec{\lambda} = (\lambda_1, \lambda_2, \dots, \lambda_M)$, representing sources of systematic uncertainties other than the background normalisation, such as the jet energy scale and the trigger efficiency. The likelihood function L , based on Poisson statistics, is given by

$$L = \prod_i \left(\exp[-\mu_i] \mu_i^{n_i} / n_i! \right) \prod_{k=1}^K \pi(\omega_k) \prod_{m=1}^M \pi(\lambda_m). \quad (2)$$

Here, i denotes the bin index of the chosen final state distribution, and μ_i and n_i are the expected and observed event numbers in bin i . The terms $\pi(\omega_k)$ and $\pi(\lambda_m)$ denote prior probability density functions for the background and the other nuisance parameters, representing the prior knowledge of these parameters. The Poisson expectation values μ_i can be further decomposed as

$$\mu_i = s_i(\sigma_{t\bar{t}}^{\text{vis}}, \vec{\lambda}) + \sum_{k=1}^K b_{k,i}^{\text{MC}}(\vec{\lambda}) (1 + \gamma_k \omega_k). \quad (3)$$

Here, s_i denotes the expected number of $t\bar{t}$ signal events, which depends on $\sigma_{t\bar{t}}^{\text{vis}}$ and the nuisance parameters $\vec{\lambda}$. The quantity $b_{k,i}^{\text{MC}}$ represents the nominal template prediction of background events from source k in bin i , and γ_k its estimated relative global normalisation uncertainty. In this analysis the background normalisation parameters ω_k and the other nuisance parameters λ_m are defined such that each prior can be represented by a unit normal distribution, unless mentioned otherwise.

A suitable differential distribution for the likelihood fit is the number of selected b-tagged jets in the event. The probability to reconstruct and identify one of the two b jets from the decaying $t\bar{t}$ pair is nearly independent of the probability to reconstruct and identify the other b jet. Because of the large mass of the top quark, the kinematic properties of the two b jets are determined to a large extent by the nearly independent decay topologies of the t and \bar{t} , and strong kinematic acceptance correlations arise only for extreme production topologies, such as for $t\bar{t}$ pairs with a large Lorentz boost.

Under the assumption of the independence of the probabilities to identify the b jets, it is possible to express the number of expected signal events with exactly one (s_1), and exactly two (s_2) b-tagged jets using binomial probabilities [14]:

$$s_1 = s_{e\mu} 2\epsilon_b (1 - C_b \epsilon_b), \quad (4)$$

$$s_2 = s_{e\mu} \epsilon_b^2 C_b. \quad (5)$$

Here, $s_{e\mu}$ is the total number of events after the $e\mu$ selection and can be written as $s_{e\mu} = \mathcal{L} \sigma_{t\bar{t}}^{\text{vis}} \epsilon_{e\mu}$, with \mathcal{L} being the integrated luminosity and $\epsilon_{e\mu}$ the efficiency for events to pass the $e\mu$

selection. The parameter ϵ_b comprises the total efficiency that a b jet is reconstructed within the kinematic acceptance and b-tagged. The quantity C_b corrects for the small correlations between the tagging of the two b jets and can be expressed as $C_b = 4s_{e\mu}s_2/(s_1 + 2s_2)^2$.

The remaining signal events with zero or more than two b-tagged jets are considered in a third category:

$$s_0 = s_{e\mu} \left[1 - 2\epsilon_b(1 - C_b\epsilon_b) - C_b\epsilon_b^2 \right]. \quad (6)$$

In Ref. [14], two equations similar to Eqs. (4, 5) are directly solved for the $t\bar{t}$ production cross section and ϵ_b . In the present analysis, Eqs. (4, 5) are used together with Eq. (6) in the template fit. The quantities $\epsilon_{e\mu}$, ϵ_b , and C_b are directly determined from the $t\bar{t}$ signal simulation, expressing ϵ_b as $(s_1 + 2s_2)/2s_{e\mu}$, and parametrised as a function of the nuisance parameters $\vec{\lambda}$. The nominal values for the 8 TeV simulated $t\bar{t}$ signal are $\epsilon_{e\mu} = 0.51$, $\epsilon_b = 0.36$, and $C_b = 0.99$, and the values for the 7 TeV sample are similar. The use of these equations facilitates an accurate modelling of the expected signal rates as a function of the nuisance parameters, i.e. avoiding mismodelling effects that could arise from approximating the dependences as linear functions.

In order to improve the sensitivity of the fit, the events are further categorised into four classes of multiplicity of additional jets in the event (zero, one, two, and three or more additional jets). This leads, together with the three classes of b-tagged jets, to 12 different categories in total. Additional jets must be non-b-tagged jets. In case there is no additional jet, the corresponding event yields are directly used in the likelihood fit, otherwise events are further categorised into bins of the p_T of the least energetic additional jet in the event.

The signal subcategory probabilities, background rates, and values of $\epsilon_{e\mu}$, ϵ_b , and C_b are obtained from simulation and depend on the nuisance parameters $\vec{\lambda}$. Each relevant dependency of a quantity on a parameter λ_m is modelled by a second-order polynomial, that is constructed from evaluating the quantity at three values $\lambda_m = 0, 1, -1$, corresponding to the nominal value of the parameter and to ± 1 standard deviation (σ) variations. For a few sources of uncertainty, only one exact variation is possible, e.g. when there are only two variants of signal generators available that differ in a certain uncertainty source such as the matrix element calculation; in such cases, a linear function is chosen to model the dependence of the quantity on the respective λ_m . For several nuisance parameters representing systematic modelling uncertainties in the measurement, a box prior is chosen instead of the standard unit normal prior, with a value of 0.5 between -1 and $+1$ and zero elsewhere. Such priors are chosen for the following uncertainties (discussed in Section 7.2): renormalisation and factorisation scales, jet-parton matching scale, top quark p_T modelling, colour reconnection, underlying event, and matrix element generator.

The likelihood fit is finally performed using the function $\chi^2 = -2 \ln L$, where L is the likelihood function given in Eq. (2). The MINUIT [66] program is used to minimise this χ^2 as function of the free fit parameters $\sigma_{t\bar{t}}$, $\vec{\omega}$, and $\vec{\lambda}$. The fit uncertainty in $\sigma_{t\bar{t}}$ is determined using MINOS, the profile likelihood algorithm which is part of MINUIT. Figures 4 and 5 show the multi-differential distributions used in the fit. A reasonably good agreement is found between data and expectations before the fit.

Figures 6 and 7 compare the data with the simulation after the simultaneous fit at 7 and 8 TeV. The uncertainty bands are calculated taking into account the full correlation matrix. The description of the data by the simulation has improved with the fit. The best fit values of the nuisance parameters correspond to variations that are for most cases within 1σ of the prior uncertainties, about 98% of the cases. The maximum observed variation is about 1.9σ , corre-

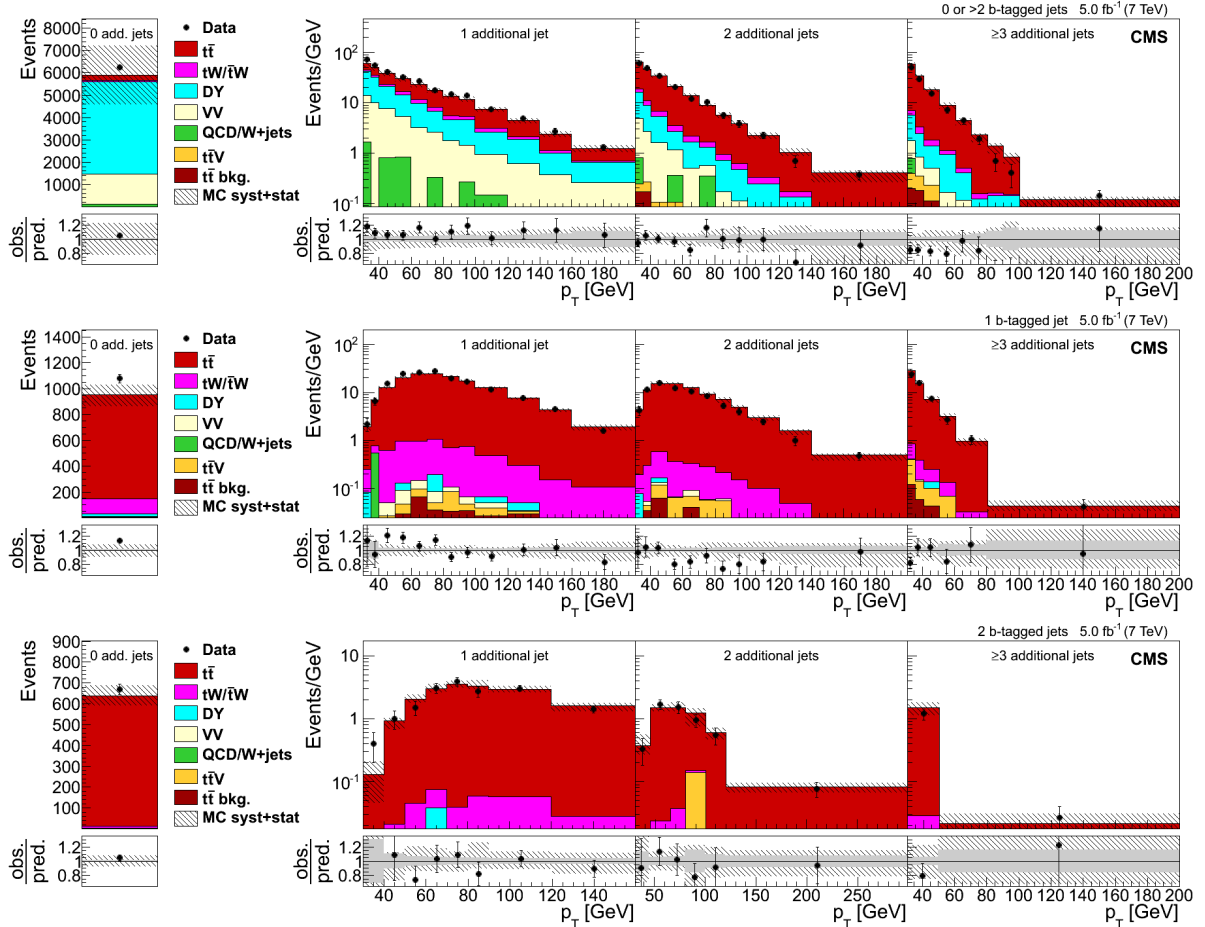


Figure 4: Total event yield for zero additional non-b-tagged jets (left) and p_T of the non-b-tagged jet with the lowest p_T in the event (right) for events with one, two, and at least three additional non-b-tagged jets, and with zero or more than two (top row), one (middle row), and two (bottom row) b-tagged jets at $\sqrt{s} = 7 \text{ TeV}$. The last bin of the p_T distributions includes the overflow events. The hatched bands correspond to the sum of statistical and systematic uncertainties in the event yield for the sum of signal and background predictions. The ratios of data to the sum of the predicted yields are shown at the bottom of each plot. Here, an additional solid grey band represents the contribution from the statistical uncertainty in the MC simulation.

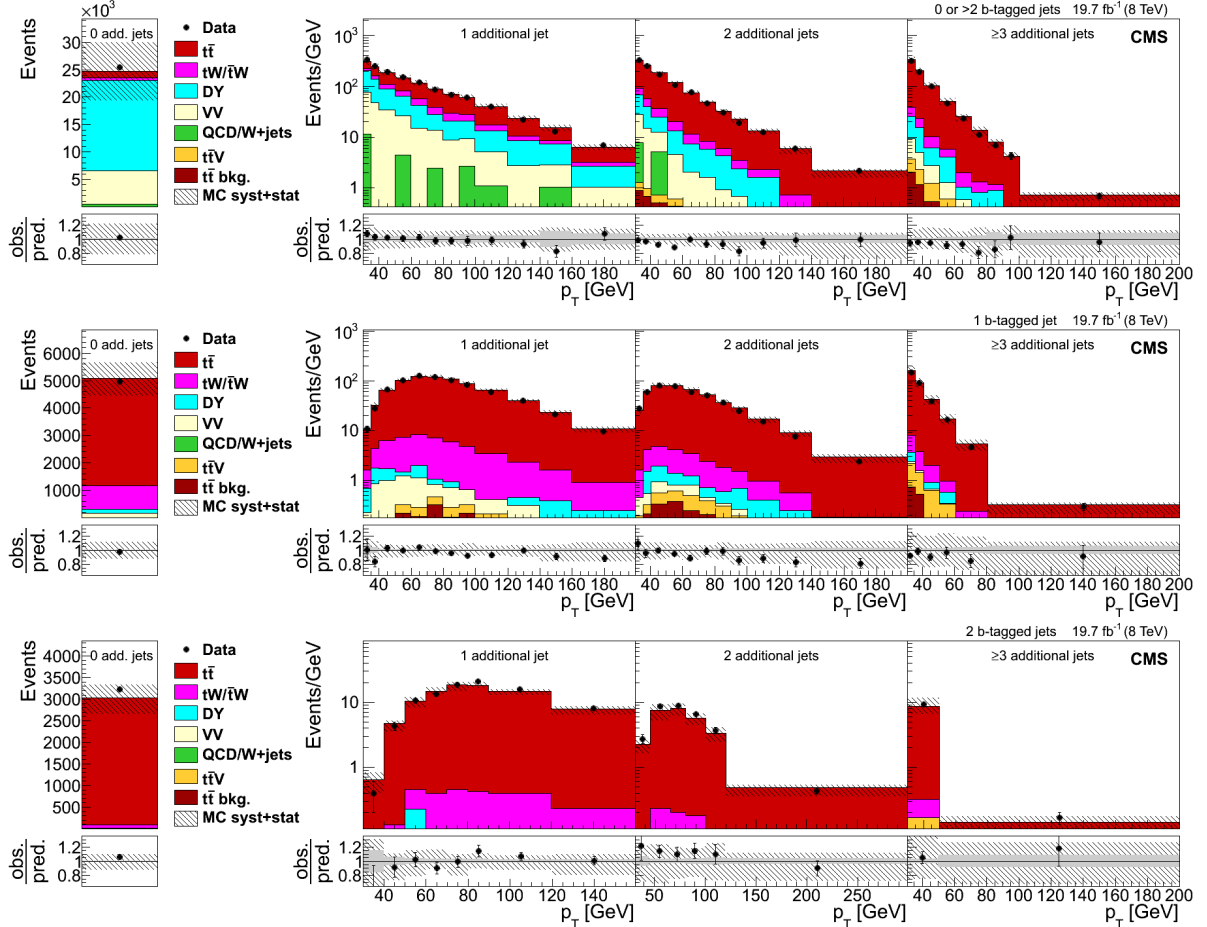


Figure 5: Total event yield for zero additional non-b-tagged jets (left) and p_T of the additional non-b-tagged jet with the lowest p_T in the event (right) for events with one, two, and at least three additional non-b-tagged jets, and with zero or more than two (top row), one (middle row), and two (bottom row) b-tagged jets at $\sqrt{s} = 8$ TeV. The last bin of the p_T distributions includes the overflow events. The hatched bands correspond to the sum of statistical and systematic uncertainties in the event yield for the sum of signal and background predictions. The ratios of data to the sum of the predicted yields are shown at the bottom of each plot. Here, an additional solid grey band represents the contribution from the statistical uncertainty in the MC simulation.

sponding to the uncertainty in the mistag SFs, see Section 7. Other uncertainties with variations between 1 and 1.5σ are two components of the jet energy scale corrections and the statistical component of the b tagging SFs.

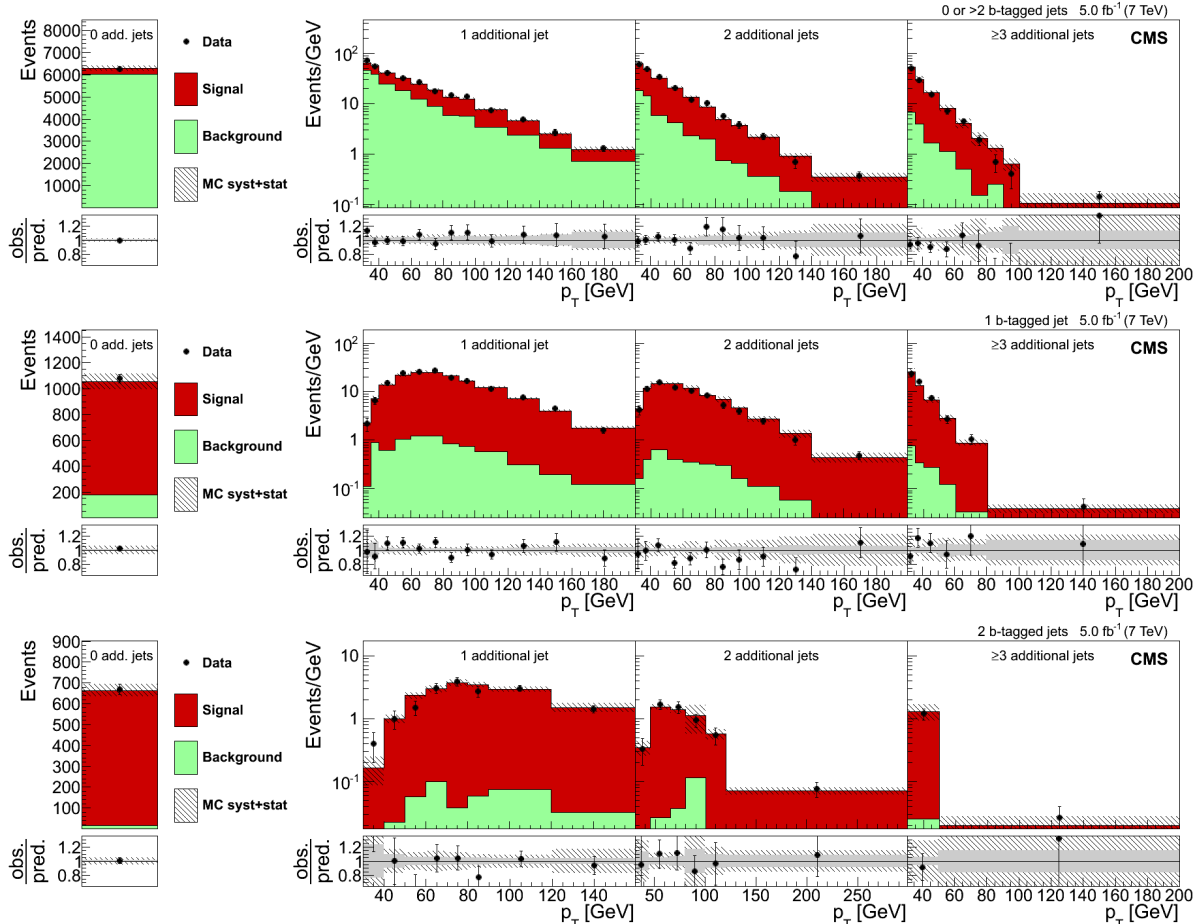


Figure 6: Fitted total event yield for zero additional non-b-tagged jets (left) and p_T of the non-b-tagged jet with the lowest p_T in the event (right) for events with one, two, and at least three additional non-b-tagged jets, and with zero or more than two (top row), one (middle row), and two (bottom row) b-tagged jets at $\sqrt{s} = 7\text{ TeV}$. The last bin of the p_T distributions includes the overflow events. The hatched bands correspond to the sum of statistical and systematic uncertainties in the event yield for the sum of signal and background predictions after the fit, and include all correlations. The ratios of data to the sum of the predicted yields are shown at the bottom of each plot. Here, an additional solid grey band represents the contribution from the statistical uncertainty in the MC simulation.

The fiducial $t\bar{t}$ production cross sections at $\sqrt{s} = 7$ and 8 TeV are determined simultaneously. For each centre-of-mass energy, a likelihood is defined as in Eq. (2), respective χ^2 functions are constructed, and the sum of both χ^2 functions is minimised. Correlations between systematic uncertainties are fully taken into account (see Section 7.3).

6.2 Event counting method

The $t\bar{t}$ production cross section is also measured by applying an event counting method similar to the one used in a previous measurement [1]. This method provides a cross-check of the reference method.

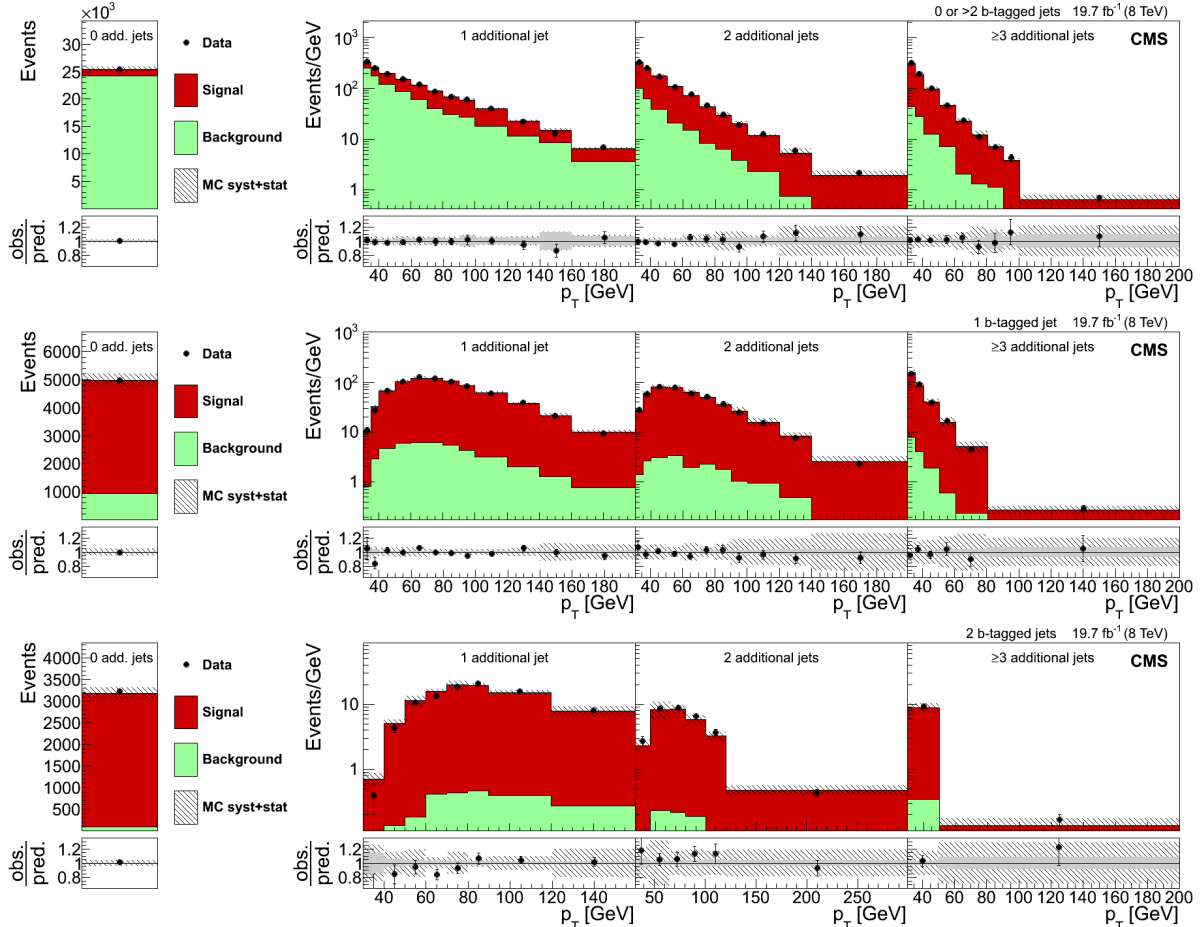


Figure 7: Fitted total event yield for zero additional non-b-tagged jets (left) and p_T of the non-b-tagged jet with the lowest p_T in the event (right) for events with one, two, and at least three additional non-b-tagged jets, and with zero or more than two (top row), one (middle row), and two (bottom row) b-tagged jets at $\sqrt{s} = 8$ TeV. The last bin of the p_T distributions includes the overflow events. The hatched bands correspond to the sum of statistical and systematic uncertainties in the event yield for the sum of signal and background predictions after the fit, and include all correlations. The ratios of data to the sum of the predicted yields are shown at the bottom of each plot. Here, an additional solid grey band represents the contribution from the statistical uncertainty in the MC simulation.

In this analysis, events are counted after applying the $e\mu$ selection described in Section 4 with additional requirements that help to further suppress the background contribution: the presence of at least two jets is required, of which at least one has to be b-tagged. Compared with Ref. [1], tighter requirements on lepton isolation and identification, as well as on b tagging, are applied to further reduce the background contribution.

Techniques based on control samples in data are used to estimate the background contribution arising from DY and from non W/Z events. The contributions of the remaining background processes are estimated from simulation. The DY contribution is estimated using the “ $R_{\text{out/in}}$ ” method [1], in which events with e^+e^- and $\mu^+\mu^-$ final states are used to obtain a normalisation factor. This is estimated from the number of events within the Z boson mass window in data, and extrapolated to the number of events outside the Z mass window with corrections based on control regions in data enriched in DY events. The contribution to the background originating from non W/Z boson events is estimated by subtracting the same-sign prompt-lepton contributions from the same-sign event yields in data and multiplying by the ratio of opposite-sign over same-sign events. This ratio, originating from non-prompt lepton backgrounds, is taken from simulation.

Table 1 shows the total number of events observed in data and the numbers of expected signal and background events fulfilling all selection criteria. For both data sets, a good agreement between data and expected number of events is observed.

Table 1: Number of selected events for the event counting method for the 7 and 8 TeV data sets. The results are given for the individual sources of background, $t\bar{t}$ signal, and data. The two uncertainties quoted correspond to the statistical and systematic components (cf. Section 7), respectively.

Source	Number of $e\mu$ events	
	7 TeV	8 TeV
DY	$22 \pm 3 \pm 3$	$173 \pm 25 \pm 26$
Non W/Z	$51 \pm 5 \pm 15$	$146 \pm 10 \pm 44$
Single top quark (tW)	$204 \pm 3 \pm 61$	$1034 \pm 3 \pm 314$
VV	$7 \pm 1 \pm 2$	$35 \pm 2 \pm 11$
$t\bar{t}V$	$12 \pm 1 \pm 3$	$84 \pm 1 \pm 26$
Total background	$296 \pm 6 \pm 63$	$1472 \pm 27 \pm 319$
$t\bar{t}$ dilepton signal	$5008 \pm 15 \pm 188$	$24440 \pm 44 \pm 956$
Data	4970	25441

Figure 8 shows the b jet multiplicity in events passing the full event selection, except for the b jet requirement, for data collected at 7 and 8 TeV. In both cases the total predicted yields provide a good description of the measured distributions.

The cross section $\sigma_{t\bar{t}}$ is determined from the number of data events after background subtraction, and dividing by the integrated luminosity of the data sample and by the product of detector and kinematical acceptance, selection efficiency, as estimated from simulation for a top quark mass of 172.5 GeV, and branching fraction of the selected $t\bar{t}$ dilepton final state.

7 Systematic uncertainties

The measurement of the top quark pair production cross section is affected by systematic uncertainties that originate from detector effects and from theoretical assumptions. Each source of systematic uncertainty is assessed individually by suitable variations of the MC simulations or

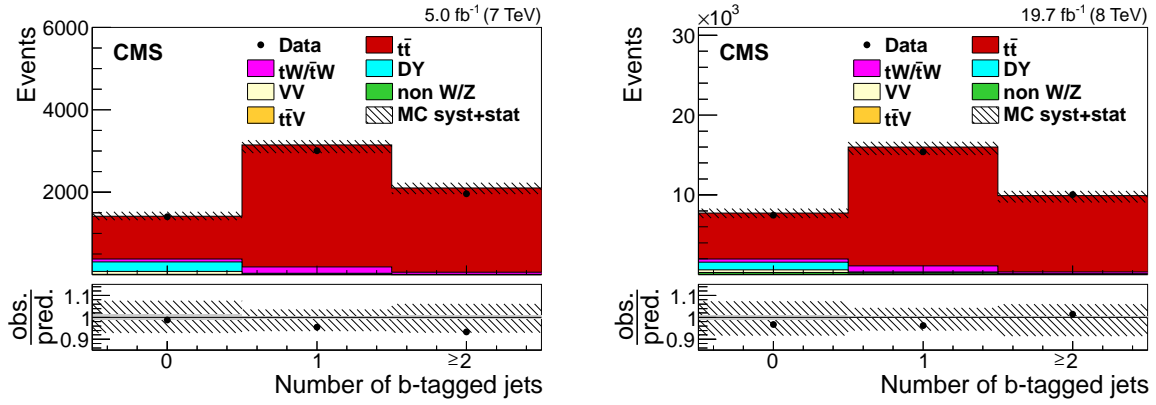


Figure 8: Comparison of the b jet multiplicity distributions in the $e\mu$ channel for 7 (left) and 8 (right) TeV between the data and simulation for events fulfilling the $e\mu$ selection and the requirement of having at least two jets. The hatched bands correspond to the sum of statistical and systematic uncertainties in the event yield for the signal and background predictions. The ratios of data to the predicted yields are shown at the bottom of each plot. Here, an additional solid grey band represents the contribution from the statistical uncertainty in the MC simulation.

by varying parameter values within their estimated uncertainties in the analysis. Each source is represented by a nuisance parameter, which is fitted together with $\sigma_{t\bar{t}}^{\text{vis}}$, as described in Section 6. For the event counting method, the same sources of systematic uncertainty are evaluated following the procedure in Ref. [1].

7.1 Experimental uncertainties

The uncertainty in the dilepton trigger (“Trigger”) and lepton identification efficiencies (“Lepton ID/isolation”) are estimated by varying the SFs within their uncertainties, which are in the range of 1–2%.

The lepton energies (“Lepton energy scale”) are corrected separately for electrons [59] and for muons [67]. Their scales are varied by 0.15% for electrons and 0.3% for muons.

The uncertainty due to the limited knowledge of the jet energy scale (“JES”) is determined by variations of the jet energy in bins of p_T and η [63]. For the reference method, these variations are divided into 27 sources and the effect of each source is evaluated individually. For the event counting method, the total variation is used to determine the uncertainty.

The uncertainty due to the limited accuracy of the jet energy resolution (“JER”) is determined by changing the simulated JER by $\pm 2.5\%$, $\pm 4\%$, and $\pm 5\%$, for jets with $|\eta| < 1.7$, $1.7 < |\eta| < 2.3$, and $|\eta| > 2.3$, respectively [63].

For the normalisation of each background source, an uncertainty of $\pm 30\%$ is assumed. In the case of the single top quark background (“ $tW/\bar{t}W$ ”), the variation covers the uncertainty in the absolute rate, including uncertainties due to PDFs. The same global variation is applied to the other dominant background contribution, DY . The predicted cross section has an uncertainty of $\approx 5\%$, including PDF uncertainties. The variation used here additionally covers the observed differences in heavy-flavour composition between data and simulation in dedicated CMS analyses and is also suggested by estimates based on data [4, 8].

The uncertainties due to the b tagging efficiency (“b tag”) and misidentification rate (“Mistag”) are determined by varying the b tagging SFs of the b jets or the light-flavour jets, respectively,

by the uncertainties quoted in Ref. [64]. For the reference method, the b tagging uncertainties are divided into 19 individual sources, some of them are correlated to other systematic uncertainties, such as JER or pileup. The remaining sources are evaluated individually.

The effect of pileup events (“Pileup”) is evaluated by weighting the inelastic pp cross section in simulation to the minimum bias cross section determined in data. The pileup model estimates the mean number of additional pp interactions to be about 9 events for the data collected at 7 TeV and 21 for the data collected at 8 TeV. These estimates are based on the total inelastic pp cross sections at $\sqrt{s} = 7$ (8) TeV, which are determined to be 73.5 (69.4) mb, following the measurement described in Ref. [68]. The systematic uncertainty is determined by varying the cross sections within their uncertainty, $\pm 8\%$ at 7 TeV and $\pm 5\%$ at 8 TeV.

The uncertainty in the luminosity (“Luminosity”) measurement is 2.2% [69] at 7 TeV and 2.6% [70] at 8 TeV.

7.2 Theoretical uncertainties

The impact of theoretical assumptions in the modelling is determined by repeating the analysis and replacing the standard MADGRAPH $t\bar{t}$ simulation by dedicated simulation samples with varied parameters.

The uncertainty in modelling of the hard-production process (“ Q^2 scale”) is assessed through a simultaneous variation of renormalisation and factorisation scales in the MADGRAPH sample by factors of 2 and 0.5 relative to their common nominal value, which is set to the $\mu_F^2 = \mu_R^2 = Q^2$ scale of the hard process. In MADGRAPH, it is defined by $Q^2 = m_t^2 + \sum p_T^2$, where the sum is over all additional final state partons in the matrix element calculations.

The impact of the choice of the scale that separates the description of jet production through matrix elements or parton shower (“ME/PS matching”) in MADGRAPH is studied by changing its reference value of 20 GeV to 40 GeV and to 10 GeV.

The effect of the matrix-element generator choice on the measurement is evaluated by using POWHEG [37, 41, 42] for the $t\bar{t}$ simulation instead of MADGRAPH (“MADGRAPH vs POWHEG”).

The flavour-dependent hadronisation uncertainty (“Hadronisation (JES)”) is part of the JES uncertainty and comes from differences in the jet energy response for different jet flavours. It is estimated by the differences between using simulations with the Lund fragmentation model in PYTHIA and cluster fragmentation model in HERWIG++ [71] and is evaluated for each jet flavour independently. An additional uncertainty included in this source is the uncertainty in the b quark fragmentation tune. This is evaluated by varying the Bowler–Lund b quark fragmentation model in tune Z2* to describe the results by ALEPH [72] and DELPHI [73] for the b quark fragmentation functions. Another uncertainty included in this source is the uncertainty in the semileptonic branching fraction of B hadrons, varied between 10.05% and 11.27%, which is the range of the measurements from B^0/B^+ decays and their uncertainties [65].

Differential cross section measurements [57] have shown that the p_T of the top quark is softer than predicted by the nominal MADGRAPH simulation used to measure the cross section. To account for this effect, the difference between the result obtained with the nominal simulation and using the MADGRAPH prediction reweighted to describe the measured top quark p_T spectrum is taken as a systematic uncertainty (“Top quark p_T modelling”).

The uncertainties from ambiguities in modelling colour reconnection effects (“Colour reconnection”) are estimated by comparing simulations of an underlying event tune including colour reconnection to a tune without it, the Perugia 2011 (P11) and P11 noCR tunes [74].

The uncertainty in the modelling of the underlying event (“Underlying event”) is estimated by evaluating the relative variations of two different P11 PYTHIA tunes with respect to the standard P11 tune: the `mpiHi` and the `TeV` tunes with higher and lower underlying event activity, respectively.

The uncertainty from the choice of PDFs (“PDF”) is determined by reweighting the sample of simulated $t\bar{t}$ events according to the 52 CT10 error PDF sets [38], scaled to 68% CL.

7.3 Correlations between systematic uncertainties for the measurements at 7 and 8 TeV

A number of systematic uncertainties affect the measurements at $\sqrt{s} = 7$ and 8 TeV similarly, while others are completely decoupled. In this analysis, systematic uncertainties are treated as either uncorrelated, partially correlated, or fully correlated between the two measurements. For fully correlated systematic uncertainties, common nuisance parameters are used in the simultaneous likelihood fit to the two data sets. For each partially correlated systematic uncertainty source, three nuisance parameters are introduced, one for each data set for the uncorrelated part and one common parameter for the correlated part. The degree of correlation is modelled by the parameter ρ . The uncertainties of the correlated and the two uncorrelated parameters are taken to be fractions ρ and $\sqrt{1 - \rho^2}$, respectively, of the uncertainty of the original nuisance parameter. The ρ values assumed for this analysis are listed in Table 2.

For experimental sources, the same procedures are usually employed at the two centre-of-mass energies for calibration and determination of uncertainties. Also, the same MC generators are used for the modelling of background processes. Hence, these uncertainties are treated as 100% correlated, however for each source a (usually small) uncorrelated component arises from statistical fluctuations in the data or simulated samples. The resulting correlation coefficients are estimated to be 0.9 for several sources and 0.8 for the “Trigger” and “Mistag” sources. For the “Pileup” source a relatively small correlation of 0.5 is assumed because of the largely different beam conditions at the two energies.

From the uncertainties related to the JES, the flavour components (“JES: flavour”), owing to the comparison between different hadronisation models, and components related to the extrapolation from $Z \rightarrow \ell\ell$ kinematic acceptance to the full phase space using MC simulation (“JES: absolute extrapolation”) are taken as fully correlated. The JES sources related to pileup (“JES: pileup”) are treated as uncorrelated, because of different procedures used for the uncertainty assessment at the two energies, as well as the remaining terms (“JES: other”). The JES component of the b tagging uncertainties is fitted independently, assigning a correlation coefficient of 0.2 that reflects the amount of correlated JES uncertainty sources.

All modelling uncertainties are assumed to be fully correlated between the two centre-of-mass energies, including the three remaining JES parts. The integrated luminosity uncertainties are treated as fully uncorrelated, to account for the different beam conditions and specific effects associated to each measurement. It has been checked that variations of the assumed correlations within reasonable ranges lead to negligible changes of the extracted cross sections.

7.4 Final uncertainties

The total uncertainties in the fiducial cross sections, as obtained with the binned likelihood fit (Section 6.1), are $^{+3.6}_{-3.4}\%$ at 7 TeV and $^{+3.7}_{-3.4}\%$ at 8 TeV. The impact of the sources of systematic uncertainties in this total uncertainty are listed in Table 3. These are estimated by removing groups of uncertainties one at a time and gauging the difference in quadrature on the total un-

Table 2: Assumed correlations ρ between systematic uncertainties for the 7 and 8 TeV data sets. If $\rho = 0$, the uncertainties are treated as uncorrelated between the two sets.

Uncertainty source	ρ
Trigger	0.8
Electron ID	0.9
Electron energy scale	0.9
Muon ID	0.9
Muon energy scale	0.9
JES: flavour	1
JES: pileup	0
JES: absolute extrapolation	1
JES: other	0
Jet energy resolution	0.9
Each background	0.9
b-tag (JES)	0.2
b-tag (stat)	0
b-tag (syst)	1
Mistag	0.8
Pileup	0.5
μ_R, μ_F scales	1
ME/PS matching	1
MADGRAPH vs POWHEG	1
b quark fragmentation tune	1
B hadron semileptonic branching fraction	1
Top quark p_T modelling	1
Colour reconnection	1
Underlying event	1
PDF	1
Integrated luminosity	0

certainty. Significant contributions to the total uncertainty spread over many different sources of experimental and modelling uncertainties with “Lumi,”, “Lepton ID/isolation”, “Trigger”, and “DY” being the four largest sources. The observed shifts of the fitted background or other nuisance parameters compared to their assumed uncertainty before the fit are in general small, indicating a consistent fit.

Table 3: Illustrative summary of the individual contributions to the total uncertainty in the visible $t\bar{t}$ cross section measurements.

Source	Uncertainty [%]	
	7 TeV	8 TeV
Trigger	1.3	1.2
Lepton ID/isolation	1.5	1.5
Lepton energy scale	0.2	0.1
Jet energy scale	0.8	0.9
Jet energy resolution	0.1	0.1
$tW/\bar{t}W$	1.0	0.6
DY	1.4	1.3
$t\bar{t}$ bkg.	0.1	0.1
$t\bar{t}V$	0.1	0.1
Diboson	0.2	0.6
$W+jets/QCD$	0.1	0.2
b-tag	0.5	0.5
Mistag	0.2	0.1
Pileup	0.3	0.3
μ_R, μ_F scales	0.3	0.6
ME/PS matching	0.1	0.1
MADGRAPH vs POWHEG	0.4	0.5
Hadronisation (JES)	0.7	0.7
Top quark p_T modelling	0.3	0.4
Colour reconnection	0.1	0.2
Underlying event	0.1	0.1
PDF	0.2	0.3
Integrated luminosity	2.2	2.6
Statistical	1.2	0.6

8 Cross section measurement

The results of the $t\bar{t}$ cross section measurements in pp collisions at 7 and 8 TeV are presented in the fiducial range and in the full phase space.

8.1 Fiducial cross section

The fiducial cross sections are defined for $t\bar{t}$ production with events containing an oppositely charged $e\mu$ pair with both leptons having $p_T > 20$ GeV and $|\eta| < 2.4$. The measured cross sections, using the binned likelihood fit extraction method (Section 6) and assuming a top quark mass of 172.5 GeV, are

$$\begin{aligned}\sigma_{t\bar{t}}^{\text{vis}} &= 3.03 \pm 0.04 \text{ (stat)}^{+0.08}_{-0.07} \text{ (syst)} \pm 0.07 \text{ (lumi)} \text{ pb,} & \text{at } \sqrt{s} = 7 \text{ TeV and} \\ \sigma_{t\bar{t}}^{\text{vis}} &= 4.23 \pm 0.02 \text{ (stat)}^{+0.11}_{-0.09} \text{ (syst)} \pm 0.11 \text{ (lumi)} \text{ pb,} & \text{at } \sqrt{s} = 8 \text{ TeV.}\end{aligned}$$

The uncertainties are due to statistical fluctuations, combined experimental and theoretical systematic effects on the measurement, and the uncertainty in the measurement of the integrated luminosity. A summary of the systematic uncertainties is presented in Table 3.

8.2 Full phase space cross section

The full phase space (total) cross sections for $t\bar{t}$ production are calculated from the fiducial cross section results by dividing $\sigma_{t\bar{t}}^{\text{vis}}$ by the acceptance, as in Eq. (1). The quantity $A_{e\mu}$ is determined from the $t\bar{t}$ signal MC simulation. As it depends on the exact theoretical model used in the event generation part of the simulation, it is parametrised as a function of the same nuisance parameters that were used for the modelling uncertainties (Section 7) in the binned likelihood fit extraction of the fiducial cross sections. The fitted values of these nuisance parameters are used to obtain the best estimates of $A_{e\mu}$, 1.745×10^{-2} at 7 TeV and 1.728×10^{-2} at 8 TeV, which are used for the determination of the nominal values of $\sigma_{t\bar{t}}$. In order to determine the uncertainty in the phase space extrapolation modelled by $A_{e\mu}$, each relevant nuisance parameter is iteratively varied from the fitted value by the $\pm 1\sigma$ values before the fit, while all other nuisance parameters are kept at their fitted values. The resulting variations of $A_{e\mu}$ are taken as an additional extrapolation uncertainty. The sources that are considered here are “ μ_R and μ_F scales”, “ME/PS matching”, “Top quark p_T modelling”, and “PDF” (see Section 7), and the individual uncertainties in $\sigma_{t\bar{t}}$ from these sources are added in quadrature. The resulting systematic uncertainties are listed in Table 4.

The measurements of $\sigma_{t\bar{t}}$ at the two centre-of-mass energies are

$$\begin{aligned}\sigma_{t\bar{t}} &= 173.6 \pm 2.1 \text{ (stat)}^{+4.5}_{-4.0} \text{ (syst)} \pm 3.8 \text{ (lumi)} \text{ pb,} & \text{at } \sqrt{s} = 7 \text{ TeV and} \\ \sigma_{t\bar{t}} &= 244.9 \pm 1.4 \text{ (stat)}^{+6.3}_{-5.5} \text{ (syst)} \pm 6.4 \text{ (lumi)} \text{ pb,} & \text{at } \sqrt{s} = 8 \text{ TeV.}\end{aligned}$$

After adding the uncertainties in quadrature, the resulting total uncertainties are 6.2 pb (3.6%) at $\sqrt{s} = 7$ TeV and 9.1 pb (3.7%) at $\sqrt{s} = 8$ TeV.

The results obtained with the method based on event counting (see Section 6.2) are

$$\begin{aligned}\sigma_{t\bar{t}} &= 165.9 \pm 2.5 \text{ (stat)} \pm 6.2 \text{ (syst)} \pm 3.6 \text{ (lumi)} \text{ pb,} & \text{at } \sqrt{s} = 7 \text{ TeV and} \\ \sigma_{t\bar{t}} &= 241.1 \pm 1.6 \text{ (stat)} \pm 10.0 \text{ (syst)} \pm 6.3 \text{ (lumi)} \text{ pb,} & \text{at } \sqrt{s} = 8 \text{ TeV.}\end{aligned}$$

As expected, the statistical and systematic uncertainties are slightly larger than those obtained with the reference method. The results of the two methods are in agreement.

Table 4: Individual contributions to the systematic uncertainty in the total $t\bar{t}$ cross section measurements. The total systematic uncertainties in the fiducial cross sections $\sigma_{t\bar{t}}^{\text{vis}}$ are given in the row “Total (visible)”, and those in the full phase space cross section $\sigma_{t\bar{t}}$ in the row “Total”.

Source	Uncertainty [%]	
	7 TeV	8 TeV
Total (visible)	+3.6 −3.4	+3.7 −3.4
Q^2 scale (extrapol.)	+0.1 −0.4	+0.2 −0.1
ME/PS matching (extrapol.)	+0.1 −0.1	+0.3 −0.3
Top quark p_T (extrapol.)	+0.5 −0.3	+0.6 −0.3
PDF (extrapol.)	+0.1 −0.1	+0.1 −0.1
Total	+3.6 −3.5	+3.7 −3.5

The cross section measurements agree with previous results [1, 4, 8, 14, 15, 21, 22]. They constitute the most precise CMS measurements of $\sigma_{t\bar{t}}$ to date and have a similar precision to the most precise ATLAS result [14], obtained in the same decay channel. For both centre-of-mass energies, the predicted cross sections at NNLO (see Section 3) are in good agreement with the measurements.

The ratio of cross sections using the results obtained with the reference analysis amounts to

$$R_{t\bar{t}} = \sigma_{t\bar{t}}(8 \text{ TeV}) / \sigma_{t\bar{t}}(7 \text{ TeV}) = 1.41 \pm 0.06.$$

Here, the correlated uncertainty obtained from the simultaneous likelihood fit (Section 6) of the fiducial cross sections at the two centre-of-mass energies is fully taken into account as well as the correlated uncertainty on the acceptances arising from model uncertainties, which are assumed to be fully correlated between the two energies. The total relative uncertainty of the ratio is 4.2%, indicating a partial cancellation of systematic uncertainties. The predicted ratio at NNLO (see Section 3) is consistent with the measurement.

9 Determination of the top quark pole mass

The full phase space cross sections are used to determine the top quark pole mass (m_t) via the dependence of the theoretically predicted cross section on m_t and comparing it to the measured cross section. For this purpose, the cross section fit and the extrapolation to the full phase space (see Sections 6 and 8.2) are repeated for three different hypotheses for the top quark mass parameter in the MC simulation (m_t^{MC}): 169.5, 172.5, and 175.5 GeV. For each mass value a sample of simulated $t\bar{t}$ events, generated with the corresponding m_t^{MC} value, is used in the fit as a signal model. The dependence of the distributions used in the fit on detector effects is evaluated individually for each mass value. Their dependence on modelling uncertainties varies little over the studied mass range and is thus taken from the nominal mass value ($m_t^{\text{MC}} = 172.5 \text{ GeV}$). The obtained cross section dependence on the mass can be parametrised as an exponential function:

$$\begin{aligned} \sigma_{t\bar{t}}(7 \text{ TeV}, m_t^{\text{MC}}) &= \exp \left[-0.1718 (m_t^{\text{MC}}/\text{GeV} - 178.5) \right] + 170.9 \text{ pb}, \\ \sigma_{t\bar{t}}(8 \text{ TeV}, m_t^{\text{MC}}) &= \exp \left[-0.1603 (m_t^{\text{MC}}/\text{GeV} - 185.4) \right] + 237.0 \text{ pb}. \end{aligned}$$

To express the measured dependence as a function of m_t instead of m_t^{MC} , the difference between m_t and m_t^{MC} needs to be accounted for. This is estimated to be of the order of 1 GeV [75]. Therefore, an additional uncertainty $\Delta_{m_t\pm}$ in the obtained cross section dependence is introduced. It is evaluated by shifting the measured dependence by ± 1 GeV in m_t^{MC} and recording the difference in $\sigma_{t\bar{t}}$. For the determination of m_t , this contribution to the total uncertainty is almost negligible. In consequence, the measurements of $\sigma_{t\bar{t}}$ can be represented by Gaussian likelihoods as a function of m_t of the form

$$L_{\text{exp}}(m_t, \sigma_{t\bar{t}}) = \exp \left[\frac{(\sigma_{t\bar{t}}(m_t) - \sigma_{t\bar{t}})^2}{-2(\Delta^2 + \Delta_{m_t\pm}^2)} \right], \quad (7)$$

where Δ represents the total uncertainty in each of the cross section measurements and $\sigma_{t\bar{t}}(m_t)$ the measured dependence of the cross section on m_t .

The predicted dependence of $\sigma_{t\bar{t}}$ on the top quark pole mass at NNLO+NNLL is determined with TOP++, employing different PDF sets (NNPDF3.0 [76], CT14 [77], and MMHT2014 [78]) with $\alpha_s = 0.118 \pm 0.001$. Additionally, uncertainties of 1.79% at 7 TeV and 1.72% at 8 TeV are assigned to the predicted cross section values to account for the uncertainty in the LHC beam energy [79]. The predicted $\sigma_{t\bar{t}}$ is represented by an asymmetric Gaussian function with width $\Delta_{p,\pm}$, comprising PDF, α_s , and the beam energy uncertainty summed in quadrature. This function is convolved with a box function to account for the uncertainty in the renormalisation and factorisation scales in the prediction [24]. The result of the convolution is given as

$$L_{\text{pred}}(m_t, \sigma_{t\bar{t}}) = \frac{1}{C(m_t)} \left(\text{erf} \left[\frac{\sigma_{t\bar{t}}^{(\text{h})}(m_t) - \sigma_{t\bar{t}}}{\sqrt{2}\Delta_{p,+}} \right] - \text{erf} \left[\frac{\sigma_{t\bar{t}}^{(\text{l})}(m_t) - \sigma_{t\bar{t}}}{\sqrt{2}\Delta_{p,-}} \right] \right), \quad (8)$$

where $\sigma_{t\bar{t}}^{(\text{h})}$ and $\sigma_{t\bar{t}}^{(\text{l})}$ denote the upper and lower predicted cross section values, respectively, from variations of the renormalisation and factorisation scales. The normalisation factor $C(m_t)$ assures that $\max(L_{\text{pred}}) = 1$ for any fixed m_t .

Figure 9 shows the likelihoods for the predicted $t\bar{t}$ cross section employing NNPDF3.0 and the measurement of $\sigma_{t\bar{t}}$ at $\sqrt{s} = 7$ and 8 TeV as a function of m_t . The product of the two likelihoods is used to fit the mass value by maximizing the likelihood simultaneously with respect to m_t and $\sigma_{t\bar{t}}$. The extracted top quark pole masses using different PDF sets are listed in Table 5. The contributions from uncertainties in the CT14 PDF set are scaled to a 68% CL.

Table 5: Top quark pole mass at NNLO+NNLL extracted by comparing the measured $t\bar{t}$ production cross section at 7 and 8 TeV with predictions employing different PDF sets.

	m_t [GeV]	
	7 TeV	8 TeV
NNPDF3.0	$173.5^{+1.9}_{-2.0}$	$174.2^{+2.0}_{-2.2}$
MMHT2014	$173.9^{+2.0}_{-2.1}$	$174.4^{+2.1}_{-2.3}$
CT14	$174.1^{+2.2}_{-2.4}$	$174.6^{+2.3}_{-2.5}$

Finally, a weighted average is calculated, taking into account all systematic uncertainty correlations between the measured cross sections at 7 and 8 TeV, and assuming 100% correlated uncertainties for the theoretical predictions at the two energies. The resulting top quark pole masses are listed in Table 6 and are in good agreement with each other and previous measurements [14, 24].

Table 6: Combined top quark pole mass at NNLO+NNLL extracted by comparing the measured $t\bar{t}$ production cross section with predictions employing different PDF sets.

	m_t [GeV]
NNPDF3.0	$173.8^{+1.7}_{-1.8}$
MMHT2014	$174.1^{+1.8}_{-2.0}$
CT14	$174.3^{+2.1}_{-2.2}$

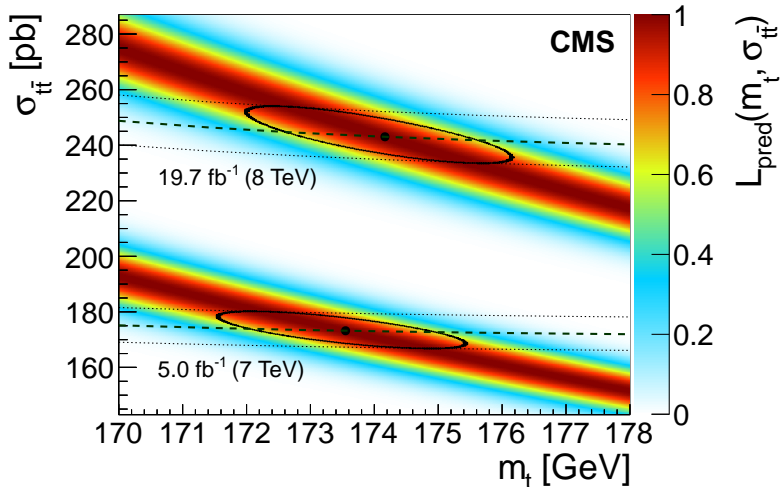


Figure 9: Likelihood for the predicted dependence of the $t\bar{t}$ production cross section on the top quark pole mass for 7 and 8 TeV determined with TOP++, employing the NNPDF3.0 PDF set. The measured dependences on the mass are given by the dashed lines, their 1σ -uncertainties are represented by the dotted lines. The extracted mass at each value of \sqrt{s} is indicated by a black point, with its 1σ -uncertainty constructed from the continuous contour, corresponding to $-2\Delta \log(L_{\text{pred}}L_{\text{exp}}) = 1$.

10 Limits on top squark pair production

The SUSY models are predicated on the existence of partners for SM particles. A light top squark could contribute to the cancellation of the quadratic divergences in the Higgs mass loop corrections [26]. SUSY scenarios with a neutralino as LSP and a nearly mass-degenerate top squark provide one theoretically possible way to account for the observed relic abundance of dark matter [80, 81]. There are therefore strong motivations to search for a top squark with a mass close to, or even below, the TeV scale.

In the following, a SUSY model with R -parity conservation is considered, where top squarks are pair-produced via the strong interaction. The top squark decays into a top quark and the LSP, considered here as the lightest neutralino $\tilde{\chi}_1^0$. A simplified model is used, where the parameters are the top squark and neutralino masses [82, 83]. The branching fraction of top squark into a top quark and a neutralino is assumed to be 100%, and the top quark polarisation is assumed to be fully right-handed. A diagram of the process is shown in Fig. 10.

Top squark pair production with the top squarks decaying into a top quark and a neutralino could produce final states very similar to the one from $t\bar{t}$ production but with additional missing transverse energy. If the difference between the masses of the top squark and the neutralino is close to the top quark mass, the events would have similar topologies to the SM $t\bar{t}$

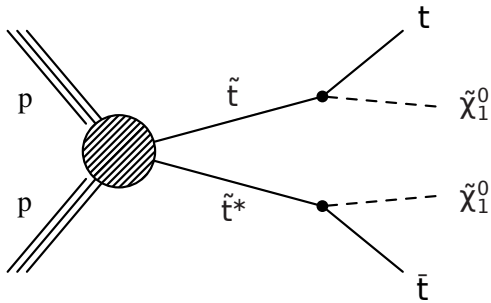


Figure 10: Diagram displaying the top squark pair production at the LHC in the decay mode where each top squark decays to a top quark and a neutralino $\tilde{\chi}_1^0$.

events. In such situations, direct top squark searches have low sensitivity because of the overwhelming $t\bar{t}$ background. However, from a very precise $t\bar{t}$ cross section measurement, top squark pair events can be searched for by looking for a small excess in the measured cross section compared to the SM expectation. The study presented here is complementary to the direct searches performed by CMS [84–86] and ATLAS [87–89], as it is more sensitive in a mass region, $m(\tilde{t}) \approx m(\tilde{\chi}_1^0) + m_t$, that is not accessible to conventional SUSY searches. Previous indirect searches in this mass region have been performed by the ATLAS collaboration [27, 90].

The 8 TeV data, analysed with the counting method (Section 6.2), are used to derive upper limits on the production cross section for the top squark pair production for different top squark masses. The number of observed events in data is compared to the sum of SM $t\bar{t}$ and background events and the expected yields from top squark pair production.

Top squark pair events generated with MADGRAPH with up to two associated partons are used for this study. The detector response is described using a fast simulation [91]. In order to account for differences with the full simulation of the CMS detector used for all other samples, a correction for the b tagging SFs is applied. Furthermore, a 10% uncertainty on the signal yields is added to account for the differences in lepton and trigger efficiencies between the fast and the full simulations. The signal samples are normalized according to the cross sections calculated at NLO+next-to-leading-logarithmic accuracy [92–96].

The 95% exclusion limits are calculated from Bayesian and modified CL_s techniques implemented in the THETA framework [97]. The yields of events given in Table 1 (where $t\bar{t}$ MC events are normalised to the predicted NNLO cross section [23, 50]) are used, accounting for all the systematic uncertainties described in Section 7. The uncertainty of 3.5% in the theoretical $t\bar{t}$ cross section is included to account for effects from renormalisation and factorisation scale and PDF uncertainties in the calculation [23].

The observed and expected limits on the mass of the top squark for neutralino masses of 1 and 12.5 GeV are shown in Fig. 11. The signal strength μ is defined as the ratio between the excluded cross section and the predicted one. Top squarks with masses below 189 GeV are excluded at 95% CL for the neutralino mass of 1 GeV, and in the range 185–189 GeV for the neutralino mass of 12.5 GeV.

The effect of the top quark polarisation on the final result is studied by calculating the exclusion limits assuming that the top quarks are 100% left-handed polarised. No significant differences are observed compared to the case of right-handed polarised top quarks.

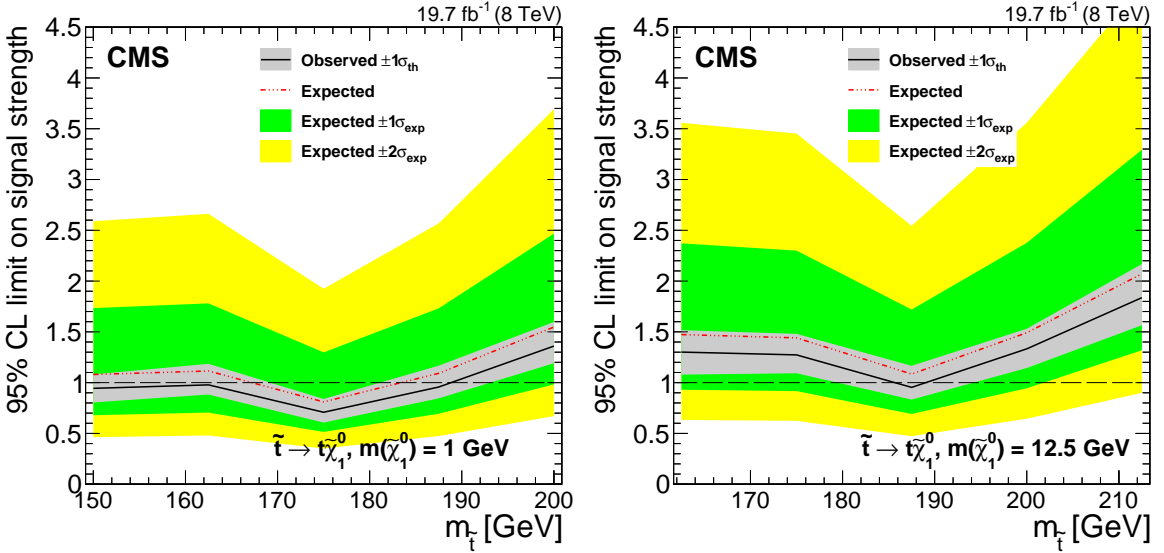


Figure 11: Expected and observed limits at 95% CL on the signal strength (see text) as a function of the top squark mass for neutralino masses of 1 GeV (left) and 12.5 GeV (right). The widest bands show the 68% and 95% CL ranges of the expected limit. The narrowest band quantifies the impact of the theoretical uncertainty in the cross section of the SUSY signal on the observed limit.

11 Summary

A measurement of the inclusive $t\bar{t}$ production cross section in proton-proton collisions at the LHC is presented using the full 2011–2012 data samples of 5.0 fb^{-1} at $\sqrt{s} = 7 \text{ TeV}$ and 19.7 fb^{-1} at $\sqrt{s} = 8 \text{ TeV}$. The analysis is performed in the $e\mu$ channel using an improved cross section extraction method. The cross sections are determined with a binned likelihood fit to the p_T distribution of the non-b-tagged jet with the lowest p_T among the selected jets in the event, using categories of number of b-tagged and additional non-b-tagged jets. Assuming a top quark mass of 172.5 GeV, the results are

$$\begin{aligned}\sigma_{t\bar{t}} &= 173.6 \pm 2.1 (\text{stat})^{+4.5}_{-4.0} (\text{syst}) \pm 3.8 (\text{lumi}) \text{ pb}, \quad \text{at } \sqrt{s} = 7 \text{ TeV and} \\ \sigma_{t\bar{t}} &= 244.9 \pm 1.4 (\text{stat})^{+6.3}_{-5.5} (\text{syst}) \pm 6.4 (\text{lumi}) \text{ pb}, \quad \text{at } \sqrt{s} = 8 \text{ TeV},\end{aligned}$$

in good agreement with recent NNLO QCD calculations. The ratio of the cross sections at the two different values of \sqrt{s} is determined to be 1.41 ± 0.06 . Moreover, the cross sections are measured in fiducial ranges defined by the transverse momentum and pseudorapidity requirements on the two charged leptons in the final state. The measurements constitute the most precise CMS results of $\sigma_{t\bar{t}}$ so far, and are competitive with recent ATLAS results [14].

The inclusive cross sections at 7 and 8 TeV are used to determine the top quark pole mass via the dependence of the theoretically predicted cross section on the mass, employing three different PDF sets. The values of the mass are consistent between the three sets. The most precise result, $173.8^{+1.7}_{-1.8} \text{ GeV}$, is obtained using the NNPDF3.0 PDF set.

The 8 TeV data are also used to constrain the cross section of pair production of supersymmetric top squarks with masses close to the top quark mass. No excess of event yields with respect to the SM prediction is found, and exclusion limits are presented as a function of the top squark mass for two different neutralino masses.

Acknowledgments

We congratulate our colleagues in the CERN accelerator departments for the excellent performance of the LHC and thank the technical and administrative staffs at CERN and at other CMS institutes for their contributions to the success of the CMS effort. In addition, we gratefully acknowledge the computing centres and personnel of the Worldwide LHC Computing Grid for delivering so effectively the computing infrastructure essential to our analyses. Finally, we acknowledge the enduring support for the construction and operation of the LHC and the CMS detector provided by the following funding agencies: the Austrian Federal Ministry of Science, Research and Economy and the Austrian Science Fund; the Belgian Fonds de la Recherche Scientifique, and Fonds voor Wetenschappelijk Onderzoek; the Brazilian Funding Agencies (CNPq, CAPES, FAPERJ, and FAPESP); the Bulgarian Ministry of Education and Science; CERN; the Chinese Academy of Sciences, Ministry of Science and Technology, and National Natural Science Foundation of China; the Colombian Funding Agency (COLCIENCIAS); the Croatian Ministry of Science, Education and Sport, and the Croatian Science Foundation; the Research Promotion Foundation, Cyprus; the Ministry of Education and Research, Estonian Research Council via IUT23-4 and IUT23-6 and European Regional Development Fund, Estonia; the Academy of Finland, Finnish Ministry of Education and Culture, and Helsinki Institute of Physics; the Institut National de Physique Nucléaire et de Physique des Particules / CNRS, and Commissariat à l'Énergie Atomique et aux Énergies Alternatives / CEA, France; the Bundesministerium für Bildung und Forschung, Deutsche Forschungsgemeinschaft, and Helmholtz-Gemeinschaft Deutscher Forschungszentren, Germany; the General Secretariat for Research and Technology, Greece; the National Scientific Research Foundation, and National Innovation Office, Hungary; the Department of Atomic Energy and the Department of Science and Technology, India; the Institute for Studies in Theoretical Physics and Mathematics, Iran; the Science Foundation, Ireland; the Istituto Nazionale di Fisica Nucleare, Italy; the Ministry of Science, ICT and Future Planning, and National Research Foundation (NRF), Republic of Korea; the Lithuanian Academy of Sciences; the Ministry of Education, and University of Malaya (Malaysia); the Mexican Funding Agencies (CINVESTAV, CONACYT, SEP, and UASLP-FAI); the Ministry of Business, Innovation and Employment, New Zealand; the Pakistan Atomic Energy Commission; the Ministry of Science and Higher Education and the National Science Centre, Poland; the Fundação para a Ciência e a Tecnologia, Portugal; JINR, Dubna; the Ministry of Education and Science of the Russian Federation, the Federal Agency of Atomic Energy of the Russian Federation, Russian Academy of Sciences, and the Russian Foundation for Basic Research; the Ministry of Education, Science and Technological Development of Serbia; the Secretaría de Estado de Investigación, Desarrollo e Innovación and Programa Consolider-Ingenio 2010, Spain; the Swiss Funding Agencies (ETH Board, ETH Zurich, PSI, SNF, UniZH, Canton Zurich, and SER); the Ministry of Science and Technology, Taipei; the Thailand Center of Excellence in Physics, the Institute for the Promotion of Teaching Science and Technology of Thailand, Special Task Force for Activating Research and the National Science and Technology Development Agency of Thailand; the Scientific and Technical Research Council of Turkey, and Turkish Atomic Energy Authority; the National Academy of Sciences of Ukraine, and State Fund for Fundamental Researches, Ukraine; the Science and Technology Facilities Council, UK; the US Department of Energy, and the US National Science Foundation.

Individuals have received support from the Marie-Curie programme and the European Research Council and EPLANET (European Union); the Leventis Foundation; the A. P. Sloan Foundation; the Alexander von Humboldt Foundation; the Belgian Federal Science Policy Office; the Fonds pour la Formation à la Recherche dans l'Industrie et dans l'Agriculture (FRIA-Belgium); the Agentschap voor Innovatie door Wetenschap en Technologie (IWT-Belgium); the

Ministry of Education, Youth and Sports (MEYS) of the Czech Republic; the Council of Science and Industrial Research, India; the HOMING PLUS programme of the Foundation for Polish Science, cofinanced from European Union, Regional Development Fund; the OPUS programme of the National Science Center (Poland); the Compagnia di San Paolo (Torino); MIUR project 20108T4XTM (Italy); the Thalis and Aristeia programmes cofinanced by EU-ESF and the Greek NSRF; the National Priorities Research Program by Qatar National Research Fund; the Programa Clarín-COFUND del Principado de Asturias; the Rachadapisek Sompot Fund for Postdoctoral Fellowship, Chulalongkorn University (Thailand); the Chulalongkorn Academic into Its 2nd Century Project Advancement Project (Thailand); and the Welch Foundation, contract C-1845.

References

- [1] CMS Collaboration, “Measurement of the $t\bar{t}$ production cross section in the dilepton channel in pp collisions at $\sqrt{s} = 8$ TeV”, *JHEP* **02** (2014) 024,
doi:[10.1007/JHEP02\(2014\)024](https://doi.org/10.1007/JHEP02(2014)024), *arXiv*:[1312.7582](https://arxiv.org/abs/1312.7582). [Erratum:
doi:[10.1007/JHEP02\(2014\)102](https://doi.org/10.1007/JHEP02(2014)102)].
- [2] CMS Collaboration, “Measurement of the $t\bar{t}$ production cross section in pp collisions at $\sqrt{s} = 8$ TeV in dilepton final states containing one τ lepton”, *Phys. Lett. B* **739** (2014) 23,
doi:[10.1016/j.physletb.2014.10.032](https://doi.org/10.1016/j.physletb.2014.10.032), *arXiv*:[1407.6643](https://arxiv.org/abs/1407.6643).
- [3] CMS Collaboration, “Measurement of the $t\bar{t}$ production cross section in the all-jets final state in pp collisions at $\sqrt{s} = 8$ TeV”, (2015). *arXiv*:[1509.06076](https://arxiv.org/abs/1509.06076). Submitted to *Eur. Phys. J. C*.
- [4] CMS Collaboration, “Measurement of the $t\bar{t}$ production cross section and the top quark mass in the dilepton channel in pp collisions at $\sqrt{s} = 7$ TeV”, *JHEP* **07** (2011) 049,
doi:[10.1007/JHEP07\(2011\)049](https://doi.org/10.1007/JHEP07(2011)049), *arXiv*:[1105.5661](https://arxiv.org/abs/1105.5661).
- [5] CMS Collaboration, “Measurement of the $t\bar{t}$ production cross section in the all-jet final state in pp collisions at $\sqrt{s} = 7$ TeV”, *JHEP* **05** (2013) 065,
doi:[10.1007/JHEP05\(2013\)065](https://doi.org/10.1007/JHEP05(2013)065), *arXiv*:[1302.0508](https://arxiv.org/abs/1302.0508).
- [6] CMS Collaboration, “Measurement of the $t\bar{t}$ production cross section in the τ +jets channel in pp collisions at $\sqrt{s} = 7$ TeV”, *Eur. Phys. J. C* **73** (2013) 2386,
doi:[10.1140/epjc/s10052-013-2386-x](https://doi.org/10.1140/epjc/s10052-013-2386-x), *arXiv*:[1301.5755](https://arxiv.org/abs/1301.5755).
- [7] CMS Collaboration, “Measurement of the $t\bar{t}$ production cross section in pp collisions at $\sqrt{s} = 7$ TeV with lepton + jets final states”, *Phys. Lett. B* **720** (2013) 83,
doi:[10.1016/j.physletb.2013.02.021](https://doi.org/10.1016/j.physletb.2013.02.021), *arXiv*:[1212.6682](https://arxiv.org/abs/1212.6682).
- [8] CMS Collaboration, “Measurement of the $t\bar{t}$ cross section in the dilepton channel in pp collisions at $\sqrt{s} = 7$ TeV”, *JHEP* **11** (2012) 067, *doi*:[10.1007/JHEP11\(2012\)067](https://doi.org/10.1007/JHEP11(2012)067),
arXiv:[1208.2671](https://arxiv.org/abs/1208.2671).
- [9] CMS Collaboration, “Measurement of the $t\bar{t}$ production cross section in pp collisions at $\sqrt{s} = 7$ TeV in dilepton final states containing a τ ”, *Phys. Rev. D* **85** (2012) 112007,
doi:[10.1103/PhysRevD.85.112007](https://doi.org/10.1103/PhysRevD.85.112007), *arXiv*:[1203.6810](https://arxiv.org/abs/1203.6810).
- [10] CMS Collaboration, “Measurement of the $t\bar{t}$ production cross section in pp collisions at 7 TeV in lepton + jets events using b-quark jet identification”, *Phys. Rev. D* **84** (2011) 092004, *doi*:[10.1103/PhysRevD.84.092004](https://doi.org/10.1103/PhysRevD.84.092004), *arXiv*:[1108.3773](https://arxiv.org/abs/1108.3773).

- [11] CMS Collaboration, “Measurement of the top-antitop production cross section in pp collisions at $\sqrt{s} = 7$ TeV using the kinematic properties of events with leptons and jets”, *Eur. Phys. J. C* **71** (2011) 1721, doi:10.1140/epjc/s10052-011-1721-3, arXiv:1106.0902.
- [12] ATLAS Collaboration, “Measurement of the top pair production cross section in 8 TeV proton-proton collisions using kinematic information in the lepton+jets final state with ATLAS”, *Phys. Rev. D* **91** (2015) 112013, doi:10.1103/PhysRevD.91.112013, arXiv:1504.04251.
- [13] ATLAS Collaboration, “Simultaneous measurements of the $t\bar{t}$, W^+W^- , and $Z/\gamma^* \rightarrow \tau\tau$ production cross-sections in pp collisions at $\sqrt{s} = 7$ TeV with the ATLAS detector”, *Phys. Rev. D* **91** (2015) 052005, doi:10.1103/PhysRevD.91.052005, arXiv:1407.0573.
- [14] ATLAS Collaboration, “Measurement of the $t\bar{t}$ production cross-section using $e\mu$ events with b-tagged jets in pp collisions at $\sqrt{s} = 7$ and 8 TeV with the ATLAS detector”, *Eur. Phys. J. C* **74** (2014) 3109, doi:10.1140/epjc/s10052-014-3109-7, arXiv:1406.5375.
- [15] ATLAS Collaboration, “Measurement of the cross section for top-quark pair production in pp collisions at $\sqrt{s} = 7$ TeV with the ATLAS detector using final states with two high- p_T leptons”, *JHEP* **05** (2012) 059, doi:10.1007/JHEP05(2012)059, arXiv:1202.4892.
- [16] ATLAS Collaboration, “Measurement of the $t\bar{t}$ production cross section in the $\tau+\text{jets}$ channel using the ATLAS detector”, *Eur. Phys. J. C* **73** (2013) 2328, doi:10.1140/epjc/s10052-013-2328-7, arXiv:1211.7205.
- [17] ATLAS Collaboration, “Measurement of the top quark pair cross section with ATLAS in pp collisions at $\sqrt{s} = 7$ TeV using final states with an electron or a muon and a hadronically decaying τ lepton”, *Phys. Lett. B* **717** (2012) 89, doi:10.1016/j.physletb.2012.09.032, arXiv:1205.2067.
- [18] ATLAS Collaboration, “Measurement of the top quark pair production cross-section with ATLAS in the single lepton channel”, *Phys. Lett. B* **711** (2012) 244, doi:10.1016/j.physletb.2012.03.083, arXiv:1201.1889.
- [19] ATLAS Collaboration, “Measurement of the top quark pair production cross section in pp collisions at $\sqrt{s} = 7$ TeV in dilepton final states with ATLAS”, *Phys. Lett. B* **707** (2012) 459, doi:10.1016/j.physletb.2011.12.055, arXiv:1108.3699.
- [20] ATLAS Collaboration, “Measurement of the top quark-pair production cross section with ATLAS in pp collisions at $\sqrt{s} = 7$ TeV”, *Eur. Phys. J. C* **71** (2011) 1577, doi:10.1140/epjc/s10052-011-1577-6, arXiv:1012.1792.
- [21] ATLAS Collaboration, “Search for new phenomena in $t\bar{t}$ events with large missing transverse momentum”, *Phys. Rev. Lett.* **108** (2012) 041805, doi:10.1103/PhysRevLett.108.041805, arXiv:1109.4725.
- [22] ATLAS Collaboration, “Search for anomalous production of prompt like-sign muon pairs and constraints on physics beyond the Standard Model”, *Phys. Rev. D* **88** (2012) 032004, doi:10.1103/PhysRevD.85.032004, arXiv:1201.1091.

- [23] M. Czakon, P. Fiedler, and A. Mitov, “The total top quark production cross-section at hadron colliders through $\mathcal{O}(\alpha_S^4)$ ”, *Phys. Rev. Lett.* **110** (2013) 252004, doi:10.1103/PhysRevLett.110.252004, arXiv:1303.6254.
- [24] CMS Collaboration, “Determination of the top-quark pole mass and strong coupling constant from the $t\bar{t}$ production cross section in pp collisions at $\sqrt{s} = 7$ TeV”, *Phys. Lett. B* **728** (2014) 496, doi:10.1016/j.physletb.2013.12.009, arXiv:1307.1907. [Corrigendum: 10.1016/j.physletb.2014.08.040].
- [25] G. R. Farrar and P. Fayet, “Phenomenology of the production, decay, and detection of new hadronic states associated with supersymmetry”, *Phys. Lett. B* **76** (1978) 575, doi:10.1016/0370-2693(78)90858-4.
- [26] H. P. Nilles, “Supersymmetry, supergravity and particle physics”, *Phys. Rept.* **110** (1984) 1, doi:10.1016/0370-1573(84)90008-5.
- [27] ATLAS Collaboration, “Measurement of spin correlation in top-antitop quark events and search for top squark pair production in pp collisions at $\sqrt{s} = 8$ TeV using the ATLAS detector”, *Phys. Rev. Lett.* **114** (2015) 142001, doi:10.1103/PhysRevLett.114.142001, arXiv:1412.4742.
- [28] CMS Collaboration, “The CMS experiment at the CERN LHC”, *JINST* **3** (2008) S08004, doi:10.1088/1748-0221/3/08/S08004.
- [29] CMS Collaboration, “Particle-flow event reconstruction in CMS and performance for jets, taus, and E_T^{miss} ”, CMS Physics Analysis Summary CMS-PAS-PFT-09-001, 2009.
- [30] CMS Collaboration, “Commissioning of the particle-flow event reconstruction with the first LHC collisions recorded in the CMS detector”, CMS Physics Analysis Summary CMS-PAS-PFT-10-001, 2010.
- [31] J. Alwall et al., “The automated computation of tree-level and next-to-leading order differential cross sections, and their matching to parton shower simulations”, *JHEP* **07** (2014) 079, doi:10.1007/JHEP07(2014)079, arXiv:1405.0301.
- [32] P. Artoisenet, R. Frederix, O. Mattelaer, and R. Rietkerk, “Automatic spin-entangled decays of heavy resonances in Monte Carlo simulations”, *JHEP* **03** (2013) 015, doi:10.1007/JHEP03(2013)015, arXiv:1212.3460.
- [33] J. Pumplin et al., “New generation of parton distributions with uncertainties from global QCD analysis”, *JHEP* **07** (2002) 012, doi:10.1088/1126-6708/2002/07/012, arXiv:hep-ph/0201195.
- [34] T. Sjöstrand, S. Mrenna, and P. Z. Skands, “PYTHIA 6.4 physics and manual”, *JHEP* **05** (2006) 026, doi:10.1088/1126-6708/2006/05/026, arXiv:hep-ph/0603175.
- [35] M. L. Mangano, M. Moretti, F. Piccinini, and M. Treccani, “Matching matrix elements and shower evolution for top-quark production in hadronic collisions”, *JHEP* **01** (2007) 013, doi:10.1088/1126-6708/2007/01/013, arXiv:hep-ph/0611129.
- [36] N. Davidson et al., “Universal interface of TAUOLA technical and physics documentation”, *Comput. Phys. Commun.* **183** (2010) 821, doi:10.1016/j.cpc.2011.12.009, arXiv:1002.0543.

- [37] S. Alioli, P. Nason, C. Oleari, and E. Re, “A general framework for implementing NLO calculations in shower Monte Carlo programs: the POWHEG BOX”, *JHEP* **06** (2010) 043, doi:10.1007/JHEP06(2010)043, arXiv:1002.2581.
- [38] H.-L. Lai et al., “New parton distributions for collider physics”, *Phys. Rev. D* **82** (2010) 074024, doi:10.1103/PhysRevD.82.074024, arXiv:1007.2241.
- [39] R. Field, “Early LHC underlying event data – findings and surprises”, in *Hadron collider physics. Proceedings, 22nd Conference, HCP 2010, Toronto, Canada, August 23-27, 2010.* 2010. arXiv:1010.3558.
- [40] GEANT4 Collaboration, “GEANT4—a simulation toolkit”, *Nucl. Instrum. Meth. A* **506** (2003) 250, doi:10.1016/S0168-9002(03)01368-8.
- [41] S. Alioli, P. Nason, C. Oleari, and E. Re, “NLO single-top production matched with shower in POWHEG: s- and t-channel contributions”, *JHEP* **09** (2009) 111, doi:10.1088/1126-6708/2009/09/111, arXiv:0907.4076. [Erratum: doi:10.1007/JHEP02(2010)011].
- [42] E. Re, “Single-top Wt-channel production matched with parton showers using the POWHEG method”, *Eur. Phys. J. C* **71** (2011) 1547, doi:10.1140/epjc/s10052-011-1547-z, arXiv:1009.2450.
- [43] R. Field, “Min-bias and the underlying event at the LHC”, *Acta Physica Polonica B* **42** (2011) 2631, doi:10.5506/APhysPolB.42.2631.
- [44] K. Melnikov and F. Petriello, “The W boson production cross section at the LHC through $\mathcal{O}(\alpha_S^2)$ ”, *Phys. Rev. Lett.* **96** (2006) 231803, doi:10.1103/PhysRevLett.96.231803, arXiv:hep-ph/0603182.
- [45] K. Melnikov and F. Petriello, “Electroweak gauge boson production at hadron colliders through $\mathcal{O}(\alpha_S^2)$ ”, *Phys. Rev. D* **74** (2006) 114017, doi:10.1103/PhysRevD.74.114017, arXiv:hep-ph/0609070.
- [46] N. Kidonakis, “Two-loop soft anomalous dimensions for single top quark associated production with W^- or H^- ”, *Phys. Rev. D* **82** (2010) 054018, doi:10.1103/PhysRevD.82.054018, arXiv:hep-ph/1005.4451.
- [47] J. M. Campbell, R. K. Ellis, and C. Williams, “Vector boson pair production at the LHC”, *JHEP* **07** (2011) 018, doi:10.1007/JHEP07(2011)018, arXiv:1105.0020.
- [48] J. M. Campbell and R. K. Ellis, “ $t\bar{t}W^\pm$ production and decay at NLO”, *JHEP* **07** (2012) 052, doi:10.1007/JHEP07(2012)052, arXiv:1204.5678.
- [49] M. V. Garzelli, A. Kardos, C. G. Papadopoulos, and Z. Trócsányi, “ $t\bar{t}W^\pm$ and $t\bar{t}Z$ hadroproduction at NLO accuracy in QCD with parton shower and hadronization effects”, *JHEP* **11** (2012) 056, doi:10.1007/JHEP11(2012)056, arXiv:1208.2665.
- [50] M. Czakon and A. Mitov, “Top++: a program for the calculation of the top-pair cross-section at hadron colliders”, *Comput. Phys. Commun.* **185** (2014) 2930, doi:10.1016/j.cpc.2014.06.021, arXiv:1112.5675.
- [51] M. Botje et al., “The PDF4LHC Working Group interim recommendations”, (2011). arXiv:1101.0538.

- [52] S. Alekhin et al., “The PDF4LHC Working Group interim report”, (2011). arXiv:1101.0536.
- [53] A. D. Martin, W. J. Stirling, R. S. Thorne, and G. Watt, “Uncertainties on α_S in global PDF analyses and implications for predicted hadronic cross sections”, *Eur. Phys. J. C* **64** (2009) 653, doi:10.1140/epjc/s10052-009-1164-2, arXiv:0905.3531.
- [54] J. Gao et al., “CT10 next-to-next-to-leading order global analysis of QCD”, *Phys. Rev. D* **89** (2014) 033009, doi:10.1103/PhysRevD.89.033009, arXiv:1302.6246.
- [55] NNPDF Collaboration, “Parton distributions with LHC data”, *Nucl. Phys. B* **867** (2013) 244, doi:10.1016/j.nuclphysb.2012.10.003, arXiv:1207.1303.
- [56] M. Czakon, M. L. Mangano, A. Mitov, and J. Rojo, “Constraints on the gluon PDF from top quark pair production at hadron colliders”, *JHEP* **07** (2013) 167, doi:10.1007/JHEP07(2013)167, arXiv:1303.7215.
- [57] CMS Collaboration, “Measurement of the differential cross section for top quark pair production in pp collisions at $\sqrt{s} = 8$ TeV”, *Eur. Phys. J. C* **75** (2015) 542, doi:10.1140/epjc/s10052-015-3709-x, arXiv:1505.04480.
- [58] CMS Collaboration, “CMS tracking performance results from early LHC operation”, *Eur. Phys. J. C* **70** (2010) 1165, doi:10.1140/epjc/s10052-010-1491-3, arXiv:1007.1988.
- [59] CMS Collaboration, “Performance of electron reconstruction and selection with the CMS detector in proton-proton collisions at $\sqrt{s} = 8$ TeV”, *JINST* **10** (2015) P06005, doi:10.1088/1748-0221/10/06/P06005, arXiv:1502.02701.
- [60] CMS Collaboration, “Performance of CMS muon reconstruction in pp collision events at $\sqrt{s} = 7$ TeV”, *JINST* **7** (2012) P10002, doi:10.1088/1748-0221/7/10/P10002, arXiv:1206.4071.
- [61] CMS Collaboration, “Measurements of inclusive W and Z cross sections in pp collisions at $\sqrt{s} = 7$ TeV”, *JHEP* **01** (2011) 080, doi:10.1007/JHEP01(2011)080, arXiv:1012.2466.
- [62] M. Cacciari, G. P. Salam, and G. Soyez, “The anti- k_t jet clustering algorithm”, *JHEP* **04** (2008) 063, doi:10.1088/1126-6708/2008/04/063, arXiv:0802.1189.
- [63] CMS Collaboration, “Determination of jet energy calibration and transverse momentum resolution in CMS”, *JINST* **6** (2011) P11002, doi:10.1088/1748-0221/6/11/P11002, arXiv:1107.4277.
- [64] CMS Collaboration, “Identification of b-quark jets with the CMS experiment”, *JINST* **8** (2013) 04013, doi:10.1088/1748-0221/8/04/P04013, arXiv:1211.4462.
- [65] Particle Data Group, K. A. Olive et al., “Review of Particle Physics”, *Chin. Phys. C* **38** (2014) 090001, doi:10.1088/1674-1137/38/9/090001.
- [66] F. James and M. Roos, “Minuit: a system for function minimization and analysis of the parameter errors and correlations”, *Comput. Phys. Commun.* **10** (1975) 343, doi:10.1016/0010-4655(75)90039-9.

- [67] A. Bodek et al., “Extracting muon momentum scale corrections for hadron collider experiments”, *Eur. Phys. J. C* **72** (2012) 2194,
`doi:10.1140/epjc/s10052-012-2194-8, arXiv:1208.3710.`
- [68] TOTEM Collaboration, “First measurement of the total proton-proton cross section at the LHC energy of $\sqrt{s} = 7 \text{ TeV}$ ”, *Europhys. Lett.* **96** (2011) 21002,
`doi:10.1209/0295-5075/96/21002, arXiv:1110.1395.`
- [69] CMS Collaboration, “Absolute calibration of the luminosity measurement at CMS: Winter 2012 update”, CMS Physics Analysis Summary CMS-PAS-SMP-12-008, 2012.
- [70] CMS Collaboration, “CMS luminosity based on pixel cluster counting — Summer 2013 update”, CMS Physics Analysis Summary CMS-PAS-LUM-13-001, 2013.
- [71] M. Bähr et al., “Herwig++ physics and manual”, *Eur. Phys. J. C* **58** (2008) 639,
`doi:10.1140/epjc/s10052-008-0798-9, arXiv:0803.0883.`
- [72] ALEPH Collaboration, “Study of the fragmentation of b quarks into B mesons at the Z peak”, *Phys. Lett. B* **512** (2001) 30, `doi:10.1016/S0370-2693(01)00690-6, arXiv:hep-ex/0106051.`
- [73] DELPHI Collaboration, “A study of the b-quark fragmentation function with the DELPHI detector at LEP I and an averaged distribution obtained at the Z pole”, *Eur. Phys. J. C* **71** (2011) 1557, `doi:10.1140/epjc/s10052-011-1557-x, arXiv:1102.4748.`
- [74] P. Z. Skands, “Tuning Monte Carlo generators: the Perugia tunes”, *Phys. Rev. D* **82** (2010) 074018, `doi:10.1103/PhysRevD.82.074018, arXiv:1005.3457.`
- [75] A. Buckley et al., “General-purpose event generators for LHC physics”, *Phys. Rept.* **504** (2011) 145, `doi:10.1016/j.physrep.2011.03.005, arXiv:1101.2599.`
- [76] NNPDF Collaboration, “Parton distributions for the LHC Run II”, *JHEP* **04** (2015) 040, `doi:10.1007/JHEP04(2015)040, arXiv:1410.8849.`
- [77] S. Dulat et al., “The CT14 global analysis of quantum chromodynamics”, (2015). `arXiv:1506.07443.`
- [78] L. A. Harland-Lang, A. D. Martin, P. Motylinski, and R. S. Thorne, “Parton distributions in the LHC era: MMHT 2014 PDFs”, *Eur. Phys. J. C* **75** (2015) 204, `doi:10.1140/epjc/s10052-015-3397-6, arXiv:1412.3989.`
- [79] J. Wenninger, “Energy calibration of the LHC beams at 4 TeV”, Technical Report CERN-ATS-2013-040, 2013.
- [80] C. Boehm, A. Djouadi, and M. Drees, “Light scalar top quarks and supersymmetric dark matter”, *Phys. Rev. D* **62** (2000) 035012, `doi:10.1103/PhysRevD.62.035012, arXiv:hep-ph/9911496.`
- [81] C. Balázs, M. Carena, and C. E. M. Wagner, “Dark matter, light stops and electroweak baryogenesis”, *Phys. Rev. D* **70** (2004) 015007, `doi:10.1103/PhysRevD.70.015007, arXiv:hep-ph/0403224.`
- [82] J. Alwall, P. Schuster, and N. Toro, “Simplified models for a first characterization of new physics at the LHC”, *Phys. Rev. D* **79** (2009) 075020, `doi:10.1103/PhysRevD.79.075020, arXiv:0810.3921.`

- [83] LHC New Physics Working Group Collaboration, “Simplified models for LHC new physics searches”, *J. Phys. G* **39** (2012) 105005, doi:10.1088/0954-3899/39/10/105005, arXiv:1105.2838.
- [84] CMS Collaboration, “Search for top-squark pair production in the single-lepton final state in pp collisions at $\sqrt{s} = 8 \text{ TeV}$ ”, *Eur. Phys. J. C* **73** (2013) 2677, doi:10.1140/epjc/s10052-013-2677-2, arXiv:1308.1586.
- [85] CMS Collaboration, “Searches for third-generation squark production in fully hadronic final states in proton-proton collisions at $\sqrt{s} = 8 \text{ TeV}$ ”, *JHEP* **06** (2015) 116, doi:10.1007/JHEP06(2015)116, arXiv:1503.08037.
- [86] CMS Collaboration, “Search for direct pair production of scalar top quarks in the single- and dilepton channels in proton-proton collisions at $\sqrt{s} = 8 \text{ TeV}$ ”, (2016). arXiv:1602.03169. Submitted to JHEP.
- [87] ATLAS Collaboration, “Search for top squark pair production in final states with one isolated lepton, jets, and missing transverse momentum in $\sqrt{s} = 8 \text{ TeV}$ pp collisions with the ATLAS detector”, *JHEP* **11** (2014) 118, doi:10.1007/JHEP11(2014)118, arXiv:1407.0583.
- [88] ATLAS Collaboration, “Search for direct pair production of the top squark in all-hadronic final states in proton-proton collisions at $\sqrt{s} = 8 \text{ TeV}$ with the ATLAS detector”, *JHEP* **09** (2014) 015, doi:10.1007/JHEP09(2014)015, arXiv:1406.1122.
- [89] ATLAS Collaboration, “Search for direct top-squark pair production in final states with two leptons in pp collisions at $\sqrt{s} = 8 \text{ TeV}$ with the ATLAS detector”, *JHEP* **06** (2014) 124, doi:10.1007/JHEP06(2014)124, arXiv:1403.4853.
- [90] ATLAS Collaboration, “ATLAS Run 1 searches for direct pair production of third-generation squarks at the Large Hadron Collider”, *Eur. Phys. J. C* **75** (2015) 510, doi:10.1140/epjc/s10052-015-3726-9, arXiv:1506.08616.
- [91] S. Abdullin et al., “The fast simulation of the CMS detector at LHC”, *J. Phys. Conf. Ser.* **331** (2011) 032049, doi:10.1088/1742-6596/331/3/032049.
- [92] W. Beenakker, R. Höpker, M. Spira, and P. M. Zerwas, “Squark and gluino production at hadron colliders”, *Nucl. Phys. B* **492** (1997) 51, doi:10.1016/S0550-3213(97)80027-2, arXiv:hep-ph/9610490.
- [93] A. Kulesza and L. Motyka, “Threshold resummation for squark-antisquark and gluino-pair production at the LHC”, *Phys. Rev. Lett.* **102** (2009) 111802, doi:10.1103/PhysRevLett.102.111802, arXiv:0807.2405.
- [94] A. Kulesza and L. Motyka, “Soft gluon resummation for the production of gluino-gluino and squark-antisquark pairs at the LHC”, *Phys. Rev. D* **80** (2009) 095004, doi:10.1103/PhysRevD.80.095004, arXiv:0905.4749.
- [95] W. Beenakker et al., “Soft-gluon resummation for squark and gluino hadroproduction”, *JHEP* **12** (2009) 041, doi:10.1088/1126-6708/2009/12/041, arXiv:0909.4418.
- [96] W. Beenakker et al., “Squark and gluino hadroproduction”, *Int. J. Mod. Phys. A* **26** (2011) 2637, doi:10.1142/S0217751X11053560, arXiv:1105.1110.
- [97] T. Müller, J. Ott, and J. Wagner-Kuhr, “THETA - a framework for template-based statistical modeling and inference”. <http://theta-framework.org>.

A The CMS Collaboration

Yerevan Physics Institute, Yerevan, Armenia
V. Khachatryan, A.M. Sirunyan, A. Tumasyan

Institut für Hochenergiephysik der OeAW, Wien, Austria

W. Adam, E. Asilar, T. Bergauer, J. Brandstetter, E. Brondolin, M. Dragicevic, J. Erö, M. Flechl, M. Friedl, R. Frühwirth¹, V.M. Ghete, C. Hartl, N. Hörmann, J. Hrubec, M. Jeitler¹, A. König, M. Krammer¹, I. Krätschmer, D. Liko, T. Matsushita, I. Mikulec, D. Rabady, N. Rad, B. Rahbaran, H. Rohringer, J. Schieck¹, J. Strauss, W. Treberer-Treberspurg, W. Waltenberger, C.-E. Wulz¹

National Centre for Particle and High Energy Physics, Minsk, Belarus

V. Mossolov, N. Shumeiko, J. Suarez Gonzalez

Universiteit Antwerpen, Antwerpen, Belgium

S. Alderweireldt, T. Cornelis, E.A. De Wolf, X. Janssen, A. Knutsson, J. Lauwers, S. Luyckx, M. Van De Klundert, H. Van Haevermaet, P. Van Mechelen, N. Van Remortel, A. Van Spilbeeck

Vrije Universiteit Brussel, Brussel, Belgium

S. Abu Zeid, F. Blekman, J. D'Hondt, N. Daci, I. De Bruyn, K. Deroover, N. Heracleous, J. Keaveney, S. Lowette, S. Moortgat, L. Moreels, A. Olbrechts, Q. Python, D. Strom, S. Tavernier, W. Van Doninck, P. Van Mulders, I. Van Parijs

Université Libre de Bruxelles, Bruxelles, Belgium

H. Brun, C. Caillol, B. Clerbaux, G. De Lentdecker, G. Fasanella, L. Favart, R. Goldouzian, A. Grebenyuk, G. Karapostoli, T. Lenzi, A. Léonard, T. Maerschalk, A. Marinov, A. Randleconde, T. Seva, C. Vander Velde, P. Vanlaer, R. Yonamine, F. Zenoni, F. Zhang²

Ghent University, Ghent, Belgium

L. Benucci, A. Cimmino, S. Crucy, D. Dobur, A. Fagot, G. Garcia, M. Gul, J. Mccartin, A.A. Ocampo Rios, D. Poyraz, D. Ryckbosch, S. Salva, R. Schöfbeck, M. Sigamani, M. Tytgat, W. Van Driessche, E. Yazgan, N. Zaganidis

Université Catholique de Louvain, Louvain-la-Neuve, Belgium

S. Basegmez, C. Beluffi³, O. Bondu, S. Brochet, G. Bruno, A. Caudron, L. Ceard, S. De Visscher, C. Delaere, M. Delcourt, D. Favart, L. Forthomme, A. Giammanco, A. Jafari, P. Jez, M. Komm, V. Lemaitre, A. Mertens, M. Musich, C. Nuttens, K. Piotrkowski, L. Quertenmont, M. Selvaggi, M. Vidal Marono

Université de Mons, Mons, Belgium

N. Belyi, G.H. Hammad

Centro Brasileiro de Pesquisas Fisicas, Rio de Janeiro, Brazil

W.L. Aldá Júnior, F.L. Alves, G.A. Alves, L. Brito, M. Correa Martins Junior, M. Hamer, C. Hensel, A. Moraes, M.E. Pol, P. Rebello Teles

Universidade do Estado do Rio de Janeiro, Rio de Janeiro, Brazil

E. Belchior Batista Das Chagas, W. Carvalho, J. Chinellato⁴, A. Custódio, E.M. Da Costa, D. De Jesus Damiao, C. De Oliveira Martins, S. Fonseca De Souza, L.M. Huertas Guativa, H. Malbouisson, D. Matos Figueiredo, C. Mora Herrera, L. Mundim, H. Nogima, W.L. Prado Da Silva, A. Santoro, A. Sznajder, E.J. Tonelli Manganote⁴, A. Vilela Pereira

Universidade Estadual Paulista ^a, Universidade Federal do ABC ^b, São Paulo, Brazil

S. Ahuja^a, C.A. Bernardes^b, A. De Souza Santos^b, S. Dogra^a, T.R. Fernandez Perez Tomei^a,

E.M. Gregores^b, P.G. Mercadante^b, C.S. Moon^{a,5}, S.F. Novaes^a, Sandra S. Padula^a, D. Romero Abad^b, J.C. Ruiz Vargas

Institute for Nuclear Research and Nuclear Energy, Sofia, Bulgaria

A. Aleksandrov, R. Hadjiiska, P. Iaydjiev, M. Rodozov, S. Stoykova, G. Sultanov, M. Vutova

University of Sofia, Sofia, Bulgaria

A. Dimitrov, I. Glushkov, L. Litov, B. Pavlov, P. Petkov

Beihang University, Beijing, China

W. Fang⁶

Institute of High Energy Physics, Beijing, China

M. Ahmad, J.G. Bian, G.M. Chen, H.S. Chen, M. Chen, T. Cheng, R. Du, C.H. Jiang, D. Leggat, R. Plestina⁷, F. Romeo, S.M. Shaheen, A. Spiezja, J. Tao, C. Wang, Z. Wang, H. Zhang

State Key Laboratory of Nuclear Physics and Technology, Peking University, Beijing, China

C. Asawatangtrakuldee, Y. Ban, Q. Li, S. Liu, Y. Mao, S.J. Qian, D. Wang, Z. Xu

Universidad de Los Andes, Bogota, Colombia

C. Avila, A. Cabrera, L.F. Chaparro Sierra, C. Florez, J.P. Gomez, B. Gomez Moreno, J.C. Sanabria

University of Split, Faculty of Electrical Engineering, Mechanical Engineering and Naval Architecture, Split, Croatia

N. Godinovic, D. Lelas, I. Puljak, P.M. Ribeiro Cipriano

University of Split, Faculty of Science, Split, Croatia

Z. Antunovic, M. Kovac

Institute Rudjer Boskovic, Zagreb, Croatia

V. Brigljevic, D. Ferencek, K. Kadija, J. Luetic, S. Micanovic, L. Sudic

University of Cyprus, Nicosia, Cyprus

A. Attikis, G. Mavromanolakis, J. Mousa, C. Nicolaou, F. Ptochos, P.A. Razis, H. Rykaczewski

Charles University, Prague, Czech Republic

M. Finger⁸, M. Finger Jr.⁸

Universidad San Francisco de Quito, Quito, Ecuador

E. Carrera Jarrin

Academy of Scientific Research and Technology of the Arab Republic of Egypt, Egyptian Network of High Energy Physics, Cairo, Egypt

A.A. Abdelalim^{9,10}, E.H. Aly Lilo¹¹, Y. Assran^{12,13}, E. El-khateeb^{11,11}, E. Salama^{13,11}

National Institute of Chemical Physics and Biophysics, Tallinn, Estonia

B. Calpas, M. Kadastik, M. Murumaa, L. Perrini, M. Raidal, A. Tiko, C. Veelken

Department of Physics, University of Helsinki, Helsinki, Finland

P. Eerola, J. Pekkanen, M. Voutilainen

Helsinki Institute of Physics, Helsinki, Finland

J. Hätkönen, V. Karimäki, R. Kinnunen, T. Lampén, K. Lassila-Perini, S. Lehti, T. Lindén, P. Luukka, T. Peltola, J. Tuominiemi, E. Tuovinen, L. Wendland

Lappeenranta University of Technology, Lappeenranta, Finland

J. Talvitie, T. Tuuva

DSM/IRFU, CEA/Saclay, Gif-sur-Yvette, France

M. Besancon, F. Couderc, M. Dejardin, D. Denegri, B. Fabbro, J.L. Faure, C. Favaro, F. Ferri, S. Ganjour, A. Givernaud, P. Gras, G. Hamel de Monchenault, P. Jarry, E. Locci, M. Machet, J. Malcles, J. Rander, A. Rosowsky, M. Titov, A. Zghiche

Laboratoire Leprince-Ringuet, Ecole Polytechnique, IN2P3-CNRS, Palaiseau, France

A. Abdulsalam, I. Antropov, S. Baffioni, F. Beaudette, P. Busson, L. Cadamuro, E. Chapon, C. Charlot, O. Davignon, R. Granier de Cassagnac, M. Jo, S. Lisniak, P. Miné, I.N. Naranjo, M. Nguyen, C. Ochando, G. Ortona, P. Paganini, P. Pigard, S. Regnard, R. Salerno, Y. Sirois, T. Strebler, Y. Yilmaz, A. Zabi

Institut Pluridisciplinaire Hubert Curien, Université de Strasbourg, Université de Haute Alsace Mulhouse, CNRS/IN2P3, Strasbourg, France

J.-L. Agram¹⁴, J. Andrea, A. Aubin, D. Bloch, J.-M. Brom, M. Buttignol, E.C. Chabert, N. Chanon, C. Collard, E. Conte¹⁴, X. Coubez, J.-C. Fontaine¹⁴, D. Gelé, U. Goerlach, C. Goetzmann, A.-C. Le Bihan, J.A. Merlin¹⁵, K. Skovpen, P. Van Hove

Centre de Calcul de l’Institut National de Physique Nucléaire et de Physique des Particules, CNRS/IN2P3, Villeurbanne, France

S. Gadrat

Université de Lyon, Université Claude Bernard Lyon 1, CNRS-IN2P3, Institut de Physique Nucléaire de Lyon, Villeurbanne, France

S. Beauceron, C. Bernet, G. Boudoul, E. Bouvier, C.A. Carrillo Montoya, R. Chierici, D. Contardo, B. Courbon, P. Depasse, H. El Mamouni, J. Fan, J. Fay, S. Gascon, M. Gouzevitch, B. Ille, F. Lagarde, I.B. Laktineh, M. Lethuillier, L. Mirabito, A.L. Pequegnot, S. Perries, A. Popov¹⁶, J.D. Ruiz Alvarez, D. Sabes, V. Sordini, M. Vander Donckt, P. Verdier, S. Viret

Georgian Technical University, Tbilisi, Georgia

A. Khvedelidze⁸

Tbilisi State University, Tbilisi, Georgia

Z. Tsamalaidze⁸

RWTH Aachen University, I. Physikalisches Institut, Aachen, Germany

C. Autermann, S. Beranek, L. Feld, A. Heister, M.K. Kiesel, K. Klein, M. Lipinski, A. Ostapchuk, M. Preuten, F. Raupach, S. Schael, C. Schomakers, J.F. Schulte, J. Schulz, T. Verlage, H. Weber, V. Zhukov¹⁶

RWTH Aachen University, III. Physikalisches Institut A, Aachen, Germany

M. Ata, M. Brodski, E. Dietz-Laursonn, D. Duchardt, M. Endres, M. Erdmann, S. Erdweg, T. Esch, R. Fischer, A. Güth, T. Hebbeker, C. Heidemann, K. Hoepfner, S. Knutzen, M. Merschmeyer, A. Meyer, P. Millet, S. Mukherjee, M. Olschewski, K. Padeken, P. Papacz, T. Pook, M. Radziej, H. Reithler, M. Rieger, F. Scheuch, L. Sonnenschein, D. Teyssier, S. Thüer

RWTH Aachen University, III. Physikalisches Institut B, Aachen, Germany

V. Cherepanov, Y. Erdogan, G. Flügge, H. Geenen, M. Geisler, F. Hoehle, B. Kargoll, T. Kress, A. Künsken, J. Lingemann, A. Nehrkorn, A. Nowack, I.M. Nugent, C. Pistone, O. Pooth, A. Stahl¹⁵

Deutsches Elektronen-Synchrotron, Hamburg, Germany

M. Aldaya Martin, I. Asin, K. Beernaert, O. Behnke, U. Behrens, K. Borras¹⁷, A. Campbell, P. Connor, C. Contreras-Campana, F. Costanza, C. Diez Pardos, G. Dolinska, S. Dooling, G. Eckerlin, D. Eckstein, T. Eichhorn, E. Gallo¹⁸, J. Garay Garcia, A. Geiser, A. Gzhko,

J.M. Grados Luyando, P. Gunnellini, A. Harb, J. Hauk, M. Hempel¹⁹, H. Jung, A. Kalogeropoulos, O. Karacheban¹⁹, M. Kasemann, J. Kieseler, C. Kleinwort, I. Korol, W. Lange, A. Lelek, J. Leonard, K. Lipka, A. Lobanov, W. Lohmann¹⁹, R. Mankel, I.-A. Melzer-Pellmann, A.B. Meyer, G. Mittag, J. Mnich, A. Mussgiller, E. Ntomari, D. Pitzl, R. Placakyte, A. Raspereza, B. Roland, M.Ö. Sahin, P. Saxena, T. Schoerner-Sadenius, C. Seitz, S. Spannagel, N. Stefaniuk, K.D. Trippkewitz, G.P. Van Onsem, R. Walsh, C. Wissing

University of Hamburg, Hamburg, Germany

V. Blobel, M. Centis Vignali, A.R. Draeger, T. Dreyer, J. Erfle, E. Garutti, K. Goebel, D. Gonzalez, M. Görner, J. Haller, M. Hoffmann, R.S. Höing, A. Junkes, R. Klanner, R. Kogler, N. Kovalchuk, T. Lapsien, T. Lenz, I. Marchesini, D. Marconi, M. Meyer, M. Niedziela, D. Nowatschin, J. Ott, F. Pantaleo¹⁵, T. Peiffer, A. Perieanu, N. Pietsch, J. Poehlsen, C. Sander, C. Scharf, P. Schleper, E. Schlieckau, A. Schmidt, S. Schumann, J. Schwandt, H. Stadie, G. Steinbrück, F.M. Stober, H. Tholen, D. Troendle, E. Usai, L. Vanelderen, A. Vanhoefer, B. Vormwald

Institut für Experimentelle Kernphysik, Karlsruhe, Germany

C. Barth, C. Baus, J. Berger, C. Böser, E. Butz, T. Chwalek, F. Colombo, W. De Boer, A. Descroix, A. Dierlamm, S. Fink, F. Frensch, R. Friese, M. Giffels, A. Gilbert, D. Haitz, F. Hartmann¹⁵, S.M. Heindl, U. Husemann, I. Katkov¹⁶, A. Kornmayer¹⁵, P. Lobelle Pardo, B. Maier, H. Mildner, M.U. Mozer, T. Müller, Th. Müller, M. Plagge, G. Quast, K. Rabbertz, S. Röcker, F. Roscher, M. Schröder, G. Sieber, H.J. Simonis, R. Ulrich, J. Wagner-Kuhr, S. Wayand, M. Weber, T. Weiler, S. Williamson, C. Wöhrmann, R. Wolf

Institute of Nuclear and Particle Physics (INPP), NCSR Demokritos, Aghia Paraskevi, Greece

G. Anagnostou, G. Daskalakis, T. Geralis, V.A. Giakoumopoulou, A. Kyriakis, D. Loukas, A. Psallidas, I. Topsis-Giotis

National and Kapodistrian University of Athens, Athens, Greece

A. Agapitos, S. Kesisoglou, A. Panagiotou, N. Saoulidou, E. Tziaferi

University of Ioánnina, Ioánnina, Greece

I. Evangelou, G. Flouris, C. Foudas, P. Kokkas, N. Loukas, N. Manthos, I. Papadopoulos, E. Paradas, J. Strologas

MTA-ELTE Lendület CMS Particle and Nuclear Physics Group, Eötvös Loránd University

N. Filipovic

Wigner Research Centre for Physics, Budapest, Hungary

G. Bencze, C. Hajdu, P. Hidas, D. Horvath²⁰, F. Sikler, V. Veszpremi, G. Vesztergombi²¹, A.J. Zsigmond

Institute of Nuclear Research ATOMKI, Debrecen, Hungary

N. Beni, S. Czellar, J. Karancsi²², J. Molnar, Z. Szillasi

University of Debrecen, Debrecen, Hungary

M. Bartók²¹, A. Makovec, P. Raics, Z.L. Trocsanyi, B. Ujvari

National Institute of Science Education and Research, Bhubaneswar, India

S. Choudhury²³, P. Mal, K. Mandal, A. Nayak, D.K. Sahoo, N. Sahoo, S.K. Swain

Panjab University, Chandigarh, India

S. Bansal, S.B. Beri, V. Bhatnagar, R. Chawla, R. Gupta, U.Bhawandeep, A.K. Kalsi, A. Kaur, M. Kaur, R. Kumar, A. Mehta, M. Mittal, J.B. Singh, G. Walia

University of Delhi, Delhi, India

Ashok Kumar, A. Bhardwaj, B.C. Choudhary, R.B. Garg, S. Keshri, A. Kumar, S. Malhotra, M. Naimuddin, N. Nishu, K. Ranjan, R. Sharma, V. Sharma

Saha Institute of Nuclear Physics, Kolkata, India

R. Bhattacharya, S. Bhattacharya, K. Chatterjee, S. Dey, S. Dutta, S. Ghosh, N. Majumdar, A. Modak, K. Mondal, S. Mukhopadhyay, S. Nandan, A. Purohit, A. Roy, D. Roy, S. Roy Chowdhury, S. Sarkar, M. Sharan

Bhabha Atomic Research Centre, Mumbai, India

R. Chudasama, D. Dutta, V. Jha, V. Kumar, A.K. Mohanty¹⁵, L.M. Pant, P. Shukla, A. Topkar

Tata Institute of Fundamental Research, Mumbai, India

T. Aziz, S. Banerjee, S. Bhowmik²⁴, R.M. Chatterjee, R.K. Dewanjee, S. Dugad, S. Ganguly, S. Ghosh, M. Guchait, A. Gurtu²⁵, Sa. Jain, G. Kole, S. Kumar, B. Mahakud, M. Maity²⁴, G. Majumder, K. Mazumdar, S. Mitra, G.B. Mohanty, B. Parida, T. Sarkar²⁴, N. Sur, B. Sutar, N. Wickramage²⁶

Indian Institute of Science Education and Research (IISER), Pune, India

S. Chauhan, S. Dube, A. Kapoor, K. Kothekar, A. Rane, S. Sharma

Institute for Research in Fundamental Sciences (IPM), Tehran, Iran

H. Bakhshiansohi, H. Behnamian, S.M. Etesami²⁷, A. Fahim²⁸, M. Khakzad, M. Mohammadi Najafabadi, M. Naseri, S. Paktnat Mehdiabadi, F. Rezaei Hosseinabadi, B. Safarzadeh²⁹, M. Zeinali

University College Dublin, Dublin, Ireland

M. Felcini, M. Grunewald

INFN Sezione di Bari ^a, Università di Bari ^b, Politecnico di Bari ^c, Bari, Italy

M. Abbrescia^{a,b}, C. Calabria^{a,b}, C. Caputo^{a,b}, A. Colaleo^a, D. Creanza^{a,c}, L. Cristella^{a,b}, N. De Filippis^{a,c}, M. De Palma^{a,b}, L. Fiore^a, G. Iaselli^{a,c}, G. Maggi^{a,c}, M. Maggi^a, G. Miniello^{a,b}, S. My^{a,b}, S. Nuzzo^{a,b}, A. Pompili^{a,b}, G. Pugliese^{a,c}, R. Radogna^{a,b}, A. Ranieri^a, G. Selvaggi^{a,b}, L. Silvestris^{a,15}, R. Venditti^{a,b}

INFN Sezione di Bologna ^a, Università di Bologna ^b, Bologna, Italy

G. Abbiendi^a, C. Battilana¹⁵, D. Bonacorsi^{a,b}, S. Braibant-Giacomelli^{a,b}, L. Brigliadori^{a,b}, R. Campanini^{a,b}, P. Capiluppi^{a,b}, A. Castro^{a,b}, F.R. Cavallo^a, S.S. Chhibra^{a,b}, G. Codispoti^{a,b}, M. Cuffiani^{a,b}, G.M. Dallavalle^a, F. Fabbri^a, A. Fanfani^{a,b}, D. Fasanella^{a,b}, P. Giacomelli^a, C. Grandi^a, L. Guiducci^{a,b}, S. Marcellini^a, G. Masetti^a, A. Montanari^a, F.L. Navarria^{a,b}, A. Perrotta^a, A.M. Rossi^{a,b}, T. Rovelli^{a,b}, G.P. Siroli^{a,b}, N. Tosi^{a,b,15}

INFN Sezione di Catania ^a, Università di Catania ^b, Catania, Italy

G. Cappello^b, M. Chiorboli^{a,b}, S. Costa^{a,b}, A. Di Mattia^a, F. Giordano^{a,b}, R. Potenza^{a,b}, A. Tricomi^{a,b}, C. Tuve^{a,b}

INFN Sezione di Firenze ^a, Università di Firenze ^b, Firenze, Italy

G. Barbagli^a, V. Ciulli^{a,b}, C. Civinini^a, R. D'Alessandro^{a,b}, E. Focardi^{a,b}, V. Gori^{a,b}, P. Lenzi^{a,b}, M. Meschini^a, S. Paoletti^a, G. Sguazzoni^a, L. Viliani^{a,b,15}

INFN Laboratori Nazionali di Frascati, Frascati, Italy

L. Benussi, S. Bianco, F. Fabbri, D. Piccolo, F. Primavera¹⁵

INFN Sezione di Genova ^a, Università di Genova ^b, Genova, Italy

V. Calvelli^{a,b}, F. Ferro^a, M. Lo Vetere^{a,b}, M.R. Monge^{a,b}, E. Robutti^a, S. Tosi^{a,b}

INFN Sezione di Milano-Bicocca ^a, Università di Milano-Bicocca ^b, Milano, Italy

L. Brianza, M.E. Dinardo^{a,b}, S. Fiorendi^{a,b}, S. Gennai^a, R. Gerosa^{a,b}, A. Ghezzi^{a,b}, P. Govoni^{a,b}, S. Malvezzi^a, R.A. Manzoni^{a,b,15}, B. Marzocchi^{a,b}, D. Menasce^a, L. Moroni^a, M. Paganoni^{a,b}, D. Pedrini^a, S. Pigazzini, S. Ragazzi^{a,b}, N. Redaelli^a, T. Tabarelli de Fatis^{a,b}

INFN Sezione di Napoli ^a, Università di Napoli 'Federico II' ^b, Napoli, Italy, Università della Basilicata ^c, Potenza, Italy, Università G. Marconi ^d, Roma, Italy

S. Buontempo^a, N. Cavallo^{a,c}, S. Di Guida^{a,d,15}, M. Esposito^{a,b}, F. Fabozzi^{a,c}, A.O.M. Iorio^{a,b}, G. Lanza^a, L. Lista^a, S. Meola^{a,d,15}, M. Merola^a, P. Paolucci^{a,15}, C. Sciacca^{a,b}, F. Thyssen

INFN Sezione di Padova ^a, Università di Padova ^b, Padova, Italy, Università di Trento ^c, Trento, Italy

P. Azzi^{a,15}, N. Bacchetta^a, L. Benato^{a,b}, D. Bisello^{a,b}, A. Boletti^{a,b}, A. Branca^{a,b}, R. Carlin^{a,b}, P. Checchia^a, M. Dall'Osso^{a,b,15}, T. Dorigo^a, U. Dosselli^a, F. Gasparini^{a,b}, U. Gasparini^{a,b}, A. Gozzelino^a, K. Kanishchev^{a,c}, S. Lacaprara^a, M. Margoni^{a,b}, A.T. Meneguzzo^{a,b}, J. Pazzini^{a,b,15}, M. Pegoraro^a, N. Pozzobon^{a,b}, P. Ronchese^{a,b}, F. Simonetto^{a,b}, E. Torassa^a, M. Tosi^{a,b}, M. Zanetti, P. Zotto^{a,b}, A. Zucchetta^{a,b,15}, G. Zumerle^{a,b}

INFN Sezione di Pavia ^a, Università di Pavia ^b, Pavia, Italy

A. Braghieri^a, A. Magnani^{a,b}, P. Montagna^{a,b}, S.P. Ratti^{a,b}, V. Re^a, C. Riccardi^{a,b}, P. Salvini^a, I. Vai^{a,b}, P. Vitulo^{a,b}

INFN Sezione di Perugia ^a, Università di Perugia ^b, Perugia, Italy

L. Alunni Solestizi^{a,b}, G.M. Bilei^a, D. Ciangottini^{a,b}, L. Fanò^{a,b}, P. Lariccia^{a,b}, R. Leonardi^{a,b}, G. Mantovani^{a,b}, M. Menichelli^a, A. Saha^a, A. Santocchia^{a,b}

INFN Sezione di Pisa ^a, Università di Pisa ^b, Scuola Normale Superiore di Pisa ^c, Pisa, Italy

K. Androsov^{a,30}, P. Azzurri^{a,15}, G. Bagliesi^a, J. Bernardini^a, T. Boccali^a, R. Castaldi^a, M.A. Ciocci^{a,30}, R. Dell'Orso^a, S. Donato^{a,c}, G. Fedi, L. Foà^{a,c†}, A. Giassi^a, M.T. Grippo^{a,30}, F. Ligabue^{a,c}, T. Lomtadze^a, L. Martini^{a,b}, A. Messineo^{a,b}, F. Palla^a, A. Rizzi^{a,b}, A. Savoy-Navarro^{a,31}, P. Spagnolo^a, R. Tenchini^a, G. Tonelli^{a,b}, A. Venturi^a, P.G. Verdini^a

INFN Sezione di Roma ^a, Università di Roma ^b, Roma, Italy

L. Barone^{a,b}, F. Cavallari^a, G. D'imperio^{a,b,15}, D. Del Re^{a,b,15}, M. Diemoz^a, S. Gelli^{a,b}, C. Jorda^a, E. Longo^{a,b}, F. Margaroli^{a,b}, P. Meridiani^a, G. Organtini^{a,b}, R. Paramatti^a, F. Preiato^{a,b}, S. Rahatlou^{a,b}, C. Rovelli^a, F. Santanastasio^{a,b}

INFN Sezione di Torino ^a, Università di Torino ^b, Torino, Italy, Università del Piemonte Orientale ^c, Novara, Italy

N. Amapane^{a,b}, R. Arcidiacono^{a,c,15}, S. Argiro^{a,b}, M. Arneodo^{a,c}, N. Bartosik^a, R. Bellan^{a,b}, C. Biino^a, N. Cartiglia^a, M. Costa^{a,b}, R. Covarelli^{a,b}, A. Degano^{a,b}, N. Demaria^a, L. Finco^{a,b}, B. Kiani^{a,b}, C. Mariotti^a, S. Maselli^a, E. Migliore^{a,b}, V. Monaco^{a,b}, E. Monteil^{a,b}, M.M. Obertino^{a,b}, L. Pacher^{a,b}, N. Pastrone^a, M. Pelliccioni^a, G.L. Pinna Angioni^{a,b}, F. Ravera^{a,b}, A. Romero^{a,b}, M. Ruspa^{a,c}, R. Sacchi^{a,b}, V. Sola^a, A. Solano^{a,b}, A. Staiano^a

INFN Sezione di Trieste ^a, Università di Trieste ^b, Trieste, Italy

S. Belforte^a, V. Candelise^{a,b}, M. Casarsa^a, F. Cossutti^a, G. Della Ricca^{a,b}, B. Gobbo^a, C. La Licata^{a,b}, A. Schizzi^{a,b}, A. Zanetti^a

Kangwon National University, Chunchon, Korea

S.K. Nam

Kyungpook National University, Daegu, Korea

D.H. Kim, G.N. Kim, M.S. Kim, D.J. Kong, S. Lee, S.W. Lee, Y.D. Oh, A. Sakharov, D.C. Son

Chonbuk National University, Jeonju, KoreaJ.A. Brochero Cifuentes, H. Kim, T.J. Kim³²**Chonnam National University, Institute for Universe and Elementary Particles, Kwangju, Korea**

S. Song

Korea University, Seoul, Korea

S. Cho, S. Choi, Y. Go, D. Gyun, B. Hong, Y. Kim, B. Lee, K. Lee, K.S. Lee, S. Lee, J. Lim, S.K. Park, Y. Roh

Seoul National University, Seoul, Korea

H.D. Yoo

University of Seoul, Seoul, Korea

M. Choi, H. Kim, H. Kim, J.H. Kim, J.S.H. Lee, I.C. Park, G. Ryu, M.S. Ryu

Sungkyunkwan University, Suwon, Korea

Y. Choi, J. Goh, D. Kim, E. Kwon, J. Lee, I. Yu

Vilnius University, Vilnius, Lithuania

V. Dudenas, A. Juodagalvis, J. Vaitkus

National Centre for Particle Physics, Universiti Malaya, Kuala Lumpur, MalaysiaI. Ahmed, Z.A. Ibrahim, J.R. Komaragiri, M.A.B. Md Ali³³, F. Mohamad Idris³⁴, W.A.T. Wan Abdullah, M.N. Yusli, Z. Zolkapli**Centro de Investigacion y de Estudios Avanzados del IPN, Mexico City, Mexico**E. Casimiro Linares, H. Castilla-Valdez, E. De La Cruz-Burelo, I. Heredia-De La Cruz³⁵, A. Hernandez-Almada, R. Lopez-Fernandez, J. Mejia Guisao, A. Sanchez-Hernandez**Universidad Iberoamericana, Mexico City, Mexico**

S. Carrillo Moreno, F. Vazquez Valencia

Benemerita Universidad Autonoma de Puebla, Puebla, Mexico

I. Pedraza, H.A. Salazar Ibarguen, C. Uribe Estrada

Universidad Autónoma de San Luis Potosí, San Luis Potosí, Mexico

A. Morelos Pineda

University of Auckland, Auckland, New Zealand

D. Kofcheck

University of Canterbury, Christchurch, New Zealand

P.H. Butler

National Centre for Physics, Quaid-I-Azam University, Islamabad, Pakistan

A. Ahmad, M. Ahmad, Q. Hassan, H.R. Hoorani, W.A. Khan, T. Khurshid, M. Shoaib, M. Waqas

National Centre for Nuclear Research, Swierk, Poland

H. Bialkowska, M. Bluj, B. Boimska, T. Frueboes, M. Górska, M. Kazana, K. Nawrocki, K. Romanowska-Rybinska, M. Szleper, P. Traczyk, P. Zalewski

Institute of Experimental Physics, Faculty of Physics, University of Warsaw, Warsaw, PolandG. Brona, K. Bunkowski, A. Byszuk³⁶, K. Doroba, A. Kalinowski, M. Konecki, J. Krolikowski, M. Misiura, M. Olszewski, M. Walczak

Laboratório de Instrumentação e Física Experimental de Partículas, Lisboa, Portugal

P. Bargassa, C. Beirão Da Cruz E Silva, A. Di Francesco, P. Faccioli, P.G. Ferreira Parracho, M. Gallinaro, J. Hollar, N. Leonardo, L. Lloret Iglesias, M.V. Nemallapudi, F. Nguyen, J. Rodrigues Antunes, J. Seixas, O. Toldaiev, D. Vadruccio, J. Varela, P. Vischia

Joint Institute for Nuclear Research, Dubna, Russia

S. Afanasiev, P. Bunin, M. Gavrilenco, I. Golutvin, I. Gorbunov, A. Kamenev, V. Karjavin, A. Lanev, A. Malakhov, V. Matveev^{37,38}, P. Moisenz, V. Palichik, V. Perelygin, S. Shmatov, S. Shulha, N. Skatchkov, V. Smirnov, N. Voityshin, A. Zarubin

Petersburg Nuclear Physics Institute, Gatchina (St. Petersburg), Russia

V. Golovtsov, Y. Ivanov, V. Kim³⁹, E. Kuznetsova⁴⁰, P. Levchenko, V. Murzin, V. Oreshkin, I. Smirnov, V. Sulimov, L. Uvarov, S. Vavilov, A. Vorobyev

Institute for Nuclear Research, Moscow, Russia

Yu. Andreev, A. Dermenev, S. Gninenko, N. Golubev, A. Karneyeu, M. Kirsanov, N. Krasnikov, A. Pashenkov, D. Tlisov, A. Toropin

Institute for Theoretical and Experimental Physics, Moscow, Russia

V. Epshteyn, V. Gavrilov, N. Lychkovskaya, V. Popov, I. Pozdnyakov, G. Safronov, A. Spiridonov, M. Toms, E. Vlasov, A. Zhokin

National Research Nuclear University ‘Moscow Engineering Physics Institute’ (MEPhI), Moscow, Russia

M. Chadeeva, O. Markin, E. Popova, V. Rusinov, E. Tarkovskii

P.N. Lebedev Physical Institute, Moscow, Russia

V. Andreev, M. Azarkin³⁸, I. Dremin³⁸, M. Kirakosyan, A. Leonidov³⁸, G. Mesyats, S.V. Rusakov

Skobeltsyn Institute of Nuclear Physics, Lomonosov Moscow State University, Moscow, Russia

A. Baskakov, A. Belyaev, E. Boos, V. Bunichev, M. Dubinin⁴¹, L. Dudko, A. Gribushin, V. Klyukhin, O. Kodolova, N. Korneeva, I. Loktin, I. Miagkov, S. Obraztsov, M. Perfilov, V. Savrin

State Research Center of Russian Federation, Institute for High Energy Physics, Protvino, Russia

I. Azhgirey, I. Bayshev, S. Bitioukov, V. Kachanov, A. Kalinin, D. Konstantinov, V. Krychkine, V. Petrov, R. Ryutin, A. Sobol, L. Tourtchanovitch, S. Troshin, N. Tyurin, A. Uzunian, A. Volkov

University of Belgrade, Faculty of Physics and Vinca Institute of Nuclear Sciences, Belgrade, Serbia

P. Adzic⁴², P. Cirkovic, D. Devetak, J. Milosevic, V. Rekovic

Centro de Investigaciones Energéticas Medioambientales y Tecnológicas (CIEMAT), Madrid, Spain

J. Alcaraz Maestre, E. Calvo, M. Cerrada, M. Chamizo Llatas, N. Colino, B. De La Cruz, A. Delgado Peris, A. Escalante Del Valle, C. Fernandez Bedoya, J.P. Fernández Ramos, J. Flix, M.C. Fouz, P. Garcia-Abia, O. Gonzalez Lopez, S. Goy Lopez, J.M. Hernandez, M.I. Josa, E. Navarro De Martino, A. Pérez-Calero Yzquierdo, J. Puerta Pelayo, A. Quintario Olmeda, I. Redondo, L. Romero, M.S. Soares

Universidad Autónoma de Madrid, Madrid, Spain

J.F. de Trocóniz, M. Missiroli, D. Moran

Universidad de Oviedo, Oviedo, Spain

J. Cuevas, J. Fernandez Menendez, S. Folgueras, I. Gonzalez Caballero, E. Palencia Cortezon¹⁵, S. Sanchez Cruz, J.M. Vizan Garcia

Instituto de Física de Cantabria (IFCA), CSIC-Universidad de Cantabria, Santander, Spain

I.J. Cabrillo, A. Calderon, J.R. Castiñeiras De Saa, E. Curras, P. De Castro Manzano, M. Fernandez, J. Garcia-Ferrero, G. Gomez, A. Lopez Virto, J. Marco, R. Marco, C. Martinez Rivero, F. Matorras, J. Piedra Gomez, T. Rodrigo, A.Y. Rodríguez-Marrero, A. Ruiz-Jimeno, L. Scodellaro, N. Trevisani, I. Vila, R. Vilar Cortabitarte

CERN, European Organization for Nuclear Research, Geneva, Switzerland

D. Abbaneo, E. Auffray, G. Auzinger, M. Bachtis, P. Baillon, A.H. Ball, D. Barney, A. Benaglia, L. Benhabib, G.M. Berruti, P. Bloch, A. Bocci, A. Bonato, C. Botta, H. Breuker, T. Camporesi, R. Castello, M. Cepeda, G. Cerminara, M. D'Alfonso, D. d'Enterria, A. Dabrowski, V. Daponte, A. David, M. De Gruttola, F. De Guio, A. De Roeck, E. Di Marco⁴³, M. Dobson, M. Dordevic, B. Dorney, T. du Pree, D. Duggan, M. Dünser, N. Dupont, A. Elliott-Peisert, G. Franzoni, J. Fulcher, W. Funk, D. Gigi, K. Gill, M. Girone, F. Glege, R. Guida, S. Gundacker, M. Guthoff, J. Hammer, P. Harris, J. Hegeman, V. Innocente, P. Janot, H. Kirschenmann, V. Knünz, M.J. Kortelainen, K. Kousouris, P. Lecoq, C. Lourenço, M.T. Lucchini, N. Magini, L. Malgeri, M. Mannelli, A. Martelli, L. Masetti, F. Meijers, S. Mersi, E. Meschi, F. Moortgat, S. Morovic, M. Mulders, H. Neugebauer, S. Orfanelli⁴⁴, L. Orsini, L. Pape, E. Perez, M. Peruzzi, A. Petrilli, G. Petrucciani, A. Pfeiffer, M. Pierini, D. Piparo, A. Racz, T. Reis, G. Rolandi⁴⁵, M. Rovere, M. Ruan, H. Sakulin, J.B. Sauvan, C. Schäfer, C. Schwick, M. Seidel, A. Sharma, P. Silva, M. Simon, P. Sphicas⁴⁶, J. Steggemann, M. Stoye, Y. Takahashi, D. Treille, A. Triossi, A. Tsirou, V. Veckalns⁴⁷, G.I. Veres²¹, N. Wardle, H.K. Wöhri, A. Zagozdzinska³⁶, W.D. Zeuner

Paul Scherrer Institut, Villigen, Switzerland

W. Bertl, K. Deiters, W. Erdmann, R. Horisberger, Q. Ingram, H.C. Kaestli, D. Kotlinski, U. Langenegger, T. Rohe

Institute for Particle Physics, ETH Zurich, Zurich, Switzerland

F. Bachmair, L. Bäni, L. Bianchini, B. Casal, G. Dissertori, M. Dittmar, M. Donegà, P. Eller, C. Grab, C. Heidegger, D. Hits, J. Hoss, G. Kasieczka, P. Lecomte[†], W. Lustermann, B. Mangano, M. Marionneau, P. Martinez Ruiz del Arbol, M. Masciovecchio, M.T. Meinhard, D. Meister, F. Micheli, P. Musella, F. Nessi-Tedaldi, F. Pandolfi, J. Pata, F. Pauss, G. Perrin, L. Perrozzi, M. Quitnat, M. Rossini, M. Schönenberger, A. Starodumov⁴⁸, M. Takahashi, V.R. Tavolaro, K. Theofilatos, R. Wallny

Universität Zürich, Zurich, Switzerland

T.K. Arrestad, C. Amsler⁴⁹, L. Caminada, M.F. Canelli, V. Chiochia, A. De Cosa, C. Galloni, A. Hinzmann, T. Hreus, B. Kilminster, C. Lange, J. Ngadiuba, D. Pinna, G. Rauco, P. Robmann, D. Salerno, Y. Yang

National Central University, Chung-Li, Taiwan

K.H. Chen, T.H. Doan, Sh. Jain, R. Khurana, M. Konyushikhin, C.M. Kuo, W. Lin, Y.J. Lu, A. Pozdnyakov, S.S. Yu

National Taiwan University (NTU), Taipei, Taiwan

Arun Kumar, P. Chang, Y.H. Chang, Y.W. Chang, Y. Chao, K.F. Chen, P.H. Chen, C. Dietz, F. Fiori, U. Grundler, W.-S. Hou, Y. Hsiung, Y.F. Liu, R.-S. Lu, M. Miñano Moya, E. Petrakou, J.f. Tsai, Y.M. Tzeng

Chulalongkorn University, Faculty of Science, Department of Physics, Bangkok, Thailand
B. Asavapibhop, K. Kovitanggoon, G. Singh, N. Srimanobhas, N. Suwonjandee

Cukurova University, Adana, Turkey

A. Adiguzel, M.N. Bakirci⁵⁰, S. Damarseckin, Z.S. Demiroglu, C. Dozen, S. Girgis, G. Gokbulut,
Y. Guler, E. Gurpinar, I. Hos, E.E. Kangal⁵¹, A. Kayis Topaksu, G. Onengut⁵², K. Ozdemir⁵³,
S. Ozturk⁵⁰, D. Sunar Cerci⁵⁴, B. Tali⁵⁴, H. Topakli⁵⁰, C. Zorbilmez

Middle East Technical University, Physics Department, Ankara, Turkey

B. Bilin, S. Bilmis, B. Isildak⁵⁵, G. Karapinar⁵⁶, M. Yalvac, M. Zeyrek

Bogazici University, Istanbul, Turkey

E. Glmez, M. Kaya⁵⁷, O. Kaya⁵⁸, E.A. Yetkin⁵⁹, T. Yetkin⁶⁰

Istanbul Technical University, Istanbul, Turkey

A. Cakir, K. Cankocak, S. Sen⁶¹, F.I. Vardarli

Institute for Scintillation Materials of National Academy of Science of Ukraine, Kharkov, Ukraine

B. Grynyov

National Scientific Center, Kharkov Institute of Physics and Technology, Kharkov, Ukraine

L. Levchuk, P. Sorokin

University of Bristol, Bristol, United Kingdom

R. Aggleton, F. Ball, L. Beck, J.J. Brooke, D. Burns, E. Clement, D. Cussans, H. Flacher,
J. Goldstein, M. Grimes, G.P. Heath, H.F. Heath, J. Jacob, L. Kreczko, C. Lucas, Z. Meng,
D.M. Newbold⁶², S. Paramesvaran, A. Poll, T. Sakuma, S. Seif El Nasr-storey, S. Senkin,
D. Smith, V.J. Smith

Rutherford Appleton Laboratory, Didcot, United Kingdom

K.W. Bell, A. Belyaev⁶³, C. Brew, R.M. Brown, L. Calligaris, D. Cieri, D.J.A. Cockerill,
J.A. Coughlan, K. Harder, S. Harper, E. Olaiya, D. Petyt, C.H. Shepherd-Themistocleous,
A. Thea, I.R. Tomalin, T. Williams, S.D. Worm

Imperial College, London, United Kingdom

M. Baber, R. Bainbridge, O. Buchmuller, A. Bundock, D. Burton, S. Casasso, M. Citron,
D. Colling, L. Corpe, P. Dauncey, G. Davies, A. De Wit, M. Della Negra, P. Dunne, A. Elwood,
D. Futyan, Y. Haddad, G. Hall, G. Iles, R. Lane, R. Lucas⁶², L. Lyons, A.-M. Magnan, S. Malik,
L. Mastrolorenzo, J. Nash, A. Nikitenko⁴⁸, J. Pela, B. Penning, M. Pesaresi, D.M. Raymond,
A. Richards, A. Rose, C. Seez, A. Tapper, K. Uchida, M. Vazquez Acosta⁶⁴, T. Virdee¹⁵, S.C. Zenz

Brunel University, Uxbridge, United Kingdom

J.E. Cole, P.R. Hobson, A. Khan, P. Kyberd, D. Leslie, I.D. Reid, P. Symonds, L. Teodorescu,
M. Turner

Baylor University, Waco, USA

A. Borzou, K. Call, J. Dittmann, K. Hatakeyama, H. Liu, N. Pastika

The University of Alabama, Tuscaloosa, USA

O. Charaf, S.I. Cooper, C. Henderson, P. Rumerio

Boston University, Boston, USA

D. Arcaro, A. Avetisyan, T. Bose, D. Gastler, D. Rankin, C. Richardson, J. Rohlf, L. Sulak, D. Zou

Brown University, Providence, USA

J. Alimena, G. Benelli, E. Berry, D. Cutts, A. Ferapontov, A. Garabedian, J. Hakala, U. Heintz, O. Jesus, E. Laird, G. Landsberg, Z. Mao, M. Narain, S. Piperov, S. Sagir, R. Syarif

University of California, Davis, Davis, USA

R. Breedon, G. Breto, M. Calderon De La Barca Sanchez, S. Chauhan, M. Chertok, J. Conway, R. Conway, P.T. Cox, R. Erbacher, G. Funk, M. Gardner, W. Ko, R. Lander, C. Mclean, M. Mulhearn, D. Pellett, J. Pilot, F. Ricci-Tam, S. Shalhout, J. Smith, M. Squires, D. Stolp, M. Tripathi, S. Wilbur, R. Yohay

University of California, Los Angeles, USA

R. Cousins, P. Everaerts, A. Florent, J. Hauser, M. Ignatenko, D. Saltzberg, E. Takasugi, V. Valuev, M. Weber

University of California, Riverside, Riverside, USA

K. Burt, R. Clare, J. Ellison, J.W. Gary, G. Hanson, J. Heilman, M. Ivova PANEVA, P. Jandir, E. Kennedy, F. Lacroix, O.R. Long, M. Malberti, M. Olmedo Negrete, A. Shrinivas, H. Wei, S. Wimpenny, B. R. Yates

University of California, San Diego, La Jolla, USA

J.G. Branson, G.B. Cerati, S. Cittolin, R.T. D'Agnolo, M. Derdzinski, A. Holzner, R. Kelley, D. Klein, J. Letts, I. Macneill, D. Olivito, S. Padhi, M. Pieri, M. Sani, V. Sharma, S. Simon, M. Tadel, A. Vartak, S. Wasserbaech⁶⁵, C. Welke, J. Wood, F. Würthwein, A. Yagil, G. Zevi Della Porta

University of California, Santa Barbara, Santa Barbara, USA

J. Bradmiller-Feld, C. Campagnari, A. Dishaw, V. Dutta, K. Flowers, M. Franco Sevilla, P. Geffert, C. George, F. Golf, L. Gouskos, J. Gran, J. Incandela, N. Mccoll, S.D. Mullin, J. Richman, D. Stuart, I. Suarez, C. West, J. Yoo

California Institute of Technology, Pasadena, USA

D. Anderson, A. Apresyan, J. Bendavid, A. Bornheim, J. Bunn, Y. Chen, J. Duarte, A. Mott, H.B. Newman, C. Pena, M. Spiropulu, J.R. Vlimant, S. Xie, R.Y. Zhu

Carnegie Mellon University, Pittsburgh, USA

M.B. Andrews, V. Azzolini, A. Calamba, B. Carlson, T. Ferguson, M. Paulini, J. Russ, M. Sun, H. Vogel, I. Vorobiev

University of Colorado Boulder, Boulder, USA

J.P. Cumalat, W.T. Ford, A. Gaz, F. Jensen, A. Johnson, M. Krohn, T. Mulholland, U. Nauenberg, K. Stenson, S.R. Wagner

Cornell University, Ithaca, USA

J. Alexander, A. Chatterjee, J. Chaves, J. Chu, S. Dittmer, N. Eggert, N. Mirman, G. Nicolas Kaufman, J.R. Patterson, A. Rinkevicius, A. Ryd, L. Skinnari, L. Soffi, W. Sun, S.M. Tan, W.D. Teo, J. Thom, J. Thompson, J. Tucker, Y. Weng, P. Wittich

Fermi National Accelerator Laboratory, Batavia, USA

S. Abdullin, M. Albrow, G. Apollinari, S. Banerjee, L.A.T. Bauerdtick, A. Beretvas, J. Berryhill, P.C. Bhat, G. Bolla, K. Burkett, J.N. Butler, H.W.K. Cheung, F. Chlebana, S. Cihangir, V.D. Elvira, I. Fisk, J. Freeman, E. Gottschalk, L. Gray, D. Green, S. Grünendahl, O. Gutsche, J. Hanlon, D. Hare, R.M. Harris, S. Hasegawa, J. Hirschauer, Z. Hu, B. Jayatilaka, S. Jindariani, M. Johnson, U. Joshi, B. Klima, B. Kreis, S. Lammel, J. Lewis, J. Linacre, D. Lincoln, R. Lipton, T. Liu, R. Lopes De Sá, J. Lykken, K. Maeshima, J.M. Marraffino, S. Maruyama, D. Mason, P. McBride,

P. Merkel, S. Mrenna, S. Nahn, C. Newman-Holmes[†], V. O'Dell, K. Pedro, O. Prokofyev, G. Rakness, E. Sexton-Kennedy, A. Soha, W.J. Spalding, L. Spiegel, S. Stoynev, N. Strobbe, L. Taylor, S. Tkaczyk, N.V. Tran, L. Uplegger, E.W. Vaandering, C. Vernieri, M. Verzocchi, R. Vidal, M. Wang, H.A. Weber, A. Whitbeck

University of Florida, Gainesville, USA

D. Acosta, P. Avery, P. Bortignon, D. Bourilkov, A. Brinkerhoff, A. Carnes, M. Carver, D. Curry, S. Das, R.D. Field, I.K. Furic, J. Konigsberg, A. Korytov, K. Kotov, P. Ma, K. Matchev, H. Mei, P. Milenovic⁶⁶, G. Mitselmakher, D. Rank, R. Rossin, L. Shchutska, M. Snowball, D. Sperka, N. Terentyev, L. Thomas, J. Wang, S. Wang, J. Yelton

Florida International University, Miami, USA

S. Linn, P. Markowitz, G. Martinez, J.L. Rodriguez

Florida State University, Tallahassee, USA

A. Ackert, J.R. Adams, T. Adams, A. Askew, S. Bein, J. Bochenek, B. Diamond, J. Haas, S. Hagopian, V. Hagopian, K.F. Johnson, A. Khatiwada, H. Prosper, M. Weinberg

Florida Institute of Technology, Melbourne, USA

M.M. Baarmann, V. Bhopatkar, S. Colafranceschi⁶⁷, M. Hohlmann, H. Kalakhety, D. Noonan, T. Roy, F. Yumiceva

University of Illinois at Chicago (UIC), Chicago, USA

M.R. Adams, L. Apanasevich, D. Berry, R.R. Betts, I. Bucinskaite, R. Cavanaugh, O. Evdokimov, L. Gauthier, C.E. Gerber, D.J. Hofman, P. Kurt, C. O'Brien, I.D. Sandoval Gonzalez, P. Turner, N. Varelas, Z. Wu, M. Zakaria, J. Zhang

The University of Iowa, Iowa City, USA

B. Bilki⁶⁸, W. Clarida, K. Dilsiz, S. Durgut, R.P. Gandajula, M. Haytmyradov, V. Khristenko, J.-P. Merlo, H. Mermerkaya⁶⁹, A. Mestvirishvili, A. Moeller, J. Nachtman, H. Ogul, Y. Onel, F. Ozok⁷⁰, A. Penzo, C. Snyder, E. Tiras, J. Wetzel, K. Yi

Johns Hopkins University, Baltimore, USA

I. Anderson, B.A. Barnett, B. Blumenfeld, A. Cocoros, N. Eminizer, D. Fehling, L. Feng, A.V. Gritsan, P. Maksimovic, M. Osherson, J. Roskes, U. Sarica, M. Swartz, M. Xiao, Y. Xin, C. You

The University of Kansas, Lawrence, USA

P. Baringer, A. Bean, C. Bruner, J. Castle, R.P. Kenny III, A. Kropivnitskaya, D. Majumder, M. Malek, W. Mcbrayer, M. Murray, S. Sanders, R. Stringer, Q. Wang

Kansas State University, Manhattan, USA

A. Ivanov, K. Kaadze, S. Khalil, M. Makouski, Y. Maravin, A. Mohammadi, L.K. Saini, N. Skhirtladze, S. Toda

Lawrence Livermore National Laboratory, Livermore, USA

D. Lange, F. Rebassoo, D. Wright

University of Maryland, College Park, USA

C. Anelli, A. Baden, O. Baron, A. Belloni, B. Calvert, S.C. Eno, C. Ferraioli, J.A. Gomez, N.J. Hadley, S. Jabeen, R.G. Kellogg, T. Kolberg, J. Kunkle, Y. Lu, A.C. Mignerey, Y.H. Shin, A. Skuja, M.B. Tonjes, S.C. Tonwar

Massachusetts Institute of Technology, Cambridge, USA

A. Apyan, R. Barbieri, A. Baty, R. Bi, K. Bierwagen, S. Brandt, W. Busza, I.A. Cali, Z. Demiragli,

L. Di Matteo, G. Gomez Ceballos, M. Goncharov, D. Gulhan, D. Hsu, Y. Iiyama, G.M. Innocenti, M. Klute, D. Kovalskyi, K. Krajczar, Y.S. Lai, Y.-J. Lee, A. Levin, P.D. Luckey, A.C. Marini, C. McGinn, C. Mironov, S. Narayanan, X. Niu, C. Paus, C. Roland, G. Roland, J. Salfeld-Nebgen, G.S.F. Stephans, K. Sumorok, K. Tatar, M. Varma, D. Velicanu, J. Veverka, J. Wang, T.W. Wang, B. Wyslouch, M. Yang, V. Zhukova

University of Minnesota, Minneapolis, USA

A.C. Benvenuti, B. Dahmes, A. Evans, A. Finkel, A. Gude, P. Hansen, S. Kalafut, S.C. Kao, K. Klapoetke, Y. Kubota, Z. Lesko, J. Mans, S. Nourbakhsh, N. Ruckstuhl, R. Rusack, N. Tambe, J. Turkewitz

University of Mississippi, Oxford, USA

J.G. Acosta, S. Oliveros

University of Nebraska-Lincoln, Lincoln, USA

E. Avdeeva, R. Bartek, K. Bloom, S. Bose, D.R. Claes, A. Dominguez, C. Fangmeier, R. Gonzalez Suarez, R. Kamaliuddin, D. Knowlton, I. Kravchenko, F. Meier, J. Monroy, F. Ratnikov, J.E. Siado, G.R. Snow, B. Stieger

State University of New York at Buffalo, Buffalo, USA

M. Alyari, J. Dolen, J. George, A. Godshalk, C. Harrington, I. Iashvili, J. Kaisen, A. Kharchilava, A. Kumar, A. Parker, S. Rappoccio, B. Roozbahani

Northeastern University, Boston, USA

G. Alverson, E. Barberis, D. Baumgartel, M. Chasco, A. Hortiangtham, A. Massironi, D.M. Morse, D. Nash, T. Orimoto, R. Teixeira De Lima, D. Trocino, R.-J. Wang, D. Wood, J. Zhang

Northwestern University, Evanston, USA

S. Bhattacharya, K.A. Hahn, A. Kubik, J.F. Low, N. Mucia, N. Odell, B. Pollack, M.H. Schmitt, K. Sung, M. Trovato, M. Velasco

University of Notre Dame, Notre Dame, USA

N. Dev, M. Hildreth, C. Jessop, D.J. Karmgard, N. Kellams, K. Lannon, N. Marinelli, F. Meng, C. Mueller, Y. Musienko³⁷, M. Planer, A. Reinsvold, R. Ruchti, N. Rupprecht, G. Smith, S. Taroni, N. Valls, M. Wayne, M. Wolf, A. Woodard

The Ohio State University, Columbus, USA

L. Antonelli, J. Brinson, B. Bylsma, L.S. Durkin, S. Flowers, A. Hart, C. Hill, R. Hughes, W. Ji, T.Y. Ling, B. Liu, W. Luo, D. Puigh, M. Rodenburg, B.L. Winer, H.W. Wulsin

Princeton University, Princeton, USA

O. Driga, P. Elmer, J. Hardenbrook, P. Hebda, S.A. Koay, P. Lujan, D. Marlow, T. Medvedeva, M. Mooney, J. Olsen, C. Palmer, P. Piroué, D. Stickland, C. Tully, A. Zuranski

University of Puerto Rico, Mayaguez, USA

S. Malik

Purdue University, West Lafayette, USA

A. Barker, V.E. Barnes, D. Benedetti, D. Bortoletto, L. Gutay, M.K. Jha, M. Jones, A.W. Jung, K. Jung, D.H. Miller, N. Neumeister, B.C. Radburn-Smith, X. Shi, I. Shipsey, D. Silvers, J. Sun, A. Svyatkovskiy, F. Wang, W. Xie, L. Xu

Purdue University Calumet, Hammond, USA

N. Parashar, J. Stupak

Rice University, Houston, USA

A. Adair, B. Akgun, Z. Chen, K.M. Ecklund, F.J.M. Geurts, M. Guilbaud, W. Li, B. Michlin, M. Northup, B.P. Padley, R. Redjimi, J. Roberts, J. Rorie, Z. Tu, J. Zabel

University of Rochester, Rochester, USA

B. Betchart, A. Bodek, P. de Barbaro, R. Demina, Y.t. Duh, Y. Eshaq, T. Ferbel, M. Galanti, A. Garcia-Bellido, J. Han, O. Hindrichs, A. Khukhunaishvili, K.H. Lo, P. Tan, M. Verzetti

Rutgers, The State University of New Jersey, Piscataway, USA

J.P. Chou, E. Contreras-Campana, Y. Gershtein, E. Halkiadakis, M. Heindl, D. Hidas, E. Hughes, S. Kaplan, R. Kunnnawalkam Elayavalli, A. Lath, K. Nash, H. Saka, S. Salur, S. Schnetzer, D. Sheffield, S. Somalwar, R. Stone, S. Thomas, P. Thomassen, M. Walker

University of Tennessee, Knoxville, USA

M. Foerster, J. Heideman, G. Riley, K. Rose, S. Spanier, K. Thapa

Texas A&M University, College Station, USA

O. Bouhali⁷¹, A. Castaneda Hernandez⁷¹, A. Celik, M. Dalchenko, M. De Mattia, A. Delgado, S. Dildick, R. Eusebi, J. Gilmore, T. Huang, T. Kamon⁷², V. Krutelyov, R. Mueller, I. Osipenkov, Y. Pakhotin, R. Patel, A. Perloff, L. Perniè, D. Rathjens, A. Rose, A. Safonov, A. Tatarinov, K.A. Ulmer

Texas Tech University, Lubbock, USA

N. Akchurin, C. Cowden, J. Damgov, C. Dragoiu, P.R. Dudero, J. Faulkner, S. Kunori, K. Lamichhane, S.W. Lee, T. Libeiro, S. Undleeb, I. Volobouev, Z. Wang

Vanderbilt University, Nashville, USA

E. Appelt, A.G. Delannoy, S. Greene, A. Gurrola, R. Janjam, W. Johns, C. Maguire, Y. Mao, A. Melo, H. Ni, P. Sheldon, S. Tuo, J. Velkovska, Q. Xu

University of Virginia, Charlottesville, USA

M.W. Arenton, P. Barria, B. Cox, B. Francis, J. Goodell, R. Hirosky, A. Ledovskoy, H. Li, C. Neu, T. Sinthuprasith, X. Sun, Y. Wang, E. Wolfe, F. Xia

Wayne State University, Detroit, USA

C. Clarke, R. Harr, P.E. Karchin, C. Kottachchi Kankamamge Don, P. Lamichhane, J. Sturdy

University of Wisconsin - Madison, Madison, WI, USA

D.A. Belknap, D. Carlsmith, S. Dasu, L. Dodd, S. Duric, B. Gomber, M. Grothe, M. Herndon, A. Hervé, P. Klabbers, A. Lanaro, A. Levine, K. Long, R. Loveless, A. Mohapatra, I. Ojalvo, T. Perry, G.A. Pierro, G. Polese, T. Ruggles, T. Sarangi, A. Savin, A. Sharma, N. Smith, W.H. Smith, D. Taylor, P. Verwilligen, N. Woods

†: Deceased

1: Also at Vienna University of Technology, Vienna, Austria

2: Also at State Key Laboratory of Nuclear Physics and Technology, Peking University, Beijing, China

3: Also at Institut Pluridisciplinaire Hubert Curien, Université de Strasbourg, Université de Haute Alsace Mulhouse, CNRS/IN2P3, Strasbourg, France

4: Also at Universidade Estadual de Campinas, Campinas, Brazil

5: Also at Centre National de la Recherche Scientifique (CNRS) - IN2P3, Paris, France

6: Also at Université Libre de Bruxelles, Bruxelles, Belgium

7: Also at Laboratoire Leprince-Ringuet, Ecole Polytechnique, IN2P3-CNRS, Palaiseau, France

8: Also at Joint Institute for Nuclear Research, Dubna, Russia

-
- 9: Also at Helwan University, Cairo, Egypt
 - 10: Now at Zewail City of Science and Technology, Zewail, Egypt
 - 11: Now at Ain Shams University, Cairo, Egypt
 - 12: Also at Suez University, Suez, Egypt
 - 13: Now at British University in Egypt, Cairo, Egypt
 - 14: Also at Université de Haute Alsace, Mulhouse, France
 - 15: Also at CERN, European Organization for Nuclear Research, Geneva, Switzerland
 - 16: Also at Skobeltsyn Institute of Nuclear Physics, Lomonosov Moscow State University, Moscow, Russia
 - 17: Also at RWTH Aachen University, III. Physikalisches Institut A, Aachen, Germany
 - 18: Also at University of Hamburg, Hamburg, Germany
 - 19: Also at Brandenburg University of Technology, Cottbus, Germany
 - 20: Also at Institute of Nuclear Research ATOMKI, Debrecen, Hungary
 - 21: Also at MTA-ELTE Lendület CMS Particle and Nuclear Physics Group, Eötvös Loránd University, Budapest, Hungary
 - 22: Also at University of Debrecen, Debrecen, Hungary
 - 23: Also at Indian Institute of Science Education and Research, Bhopal, India
 - 24: Also at University of Visva-Bharati, Santiniketan, India
 - 25: Now at King Abdulaziz University, Jeddah, Saudi Arabia
 - 26: Also at University of Ruhuna, Matara, Sri Lanka
 - 27: Also at Isfahan University of Technology, Isfahan, Iran
 - 28: Also at University of Tehran, Department of Engineering Science, Tehran, Iran
 - 29: Also at Plasma Physics Research Center, Science and Research Branch, Islamic Azad University, Tehran, Iran
 - 30: Also at Università degli Studi di Siena, Siena, Italy
 - 31: Also at Purdue University, West Lafayette, USA
 - 32: Now at Hanyang University, Seoul, Korea
 - 33: Also at International Islamic University of Malaysia, Kuala Lumpur, Malaysia
 - 34: Also at Malaysian Nuclear Agency, MOSTI, Kajang, Malaysia
 - 35: Also at Consejo Nacional de Ciencia y Tecnología, Mexico city, Mexico
 - 36: Also at Warsaw University of Technology, Institute of Electronic Systems, Warsaw, Poland
 - 37: Also at Institute for Nuclear Research, Moscow, Russia
 - 38: Now at National Research Nuclear University 'Moscow Engineering Physics Institute' (MEPhI), Moscow, Russia
 - 39: Also at St. Petersburg State Polytechnical University, St. Petersburg, Russia
 - 40: Also at University of Florida, Gainesville, USA
 - 41: Also at California Institute of Technology, Pasadena, USA
 - 42: Also at Faculty of Physics, University of Belgrade, Belgrade, Serbia
 - 43: Also at INFN Sezione di Roma; Università di Roma, Roma, Italy
 - 44: Also at National Technical University of Athens, Athens, Greece
 - 45: Also at Scuola Normale e Sezione dell'INFN, Pisa, Italy
 - 46: Also at National and Kapodistrian University of Athens, Athens, Greece
 - 47: Also at Riga Technical University, Riga, Latvia
 - 48: Also at Institute for Theoretical and Experimental Physics, Moscow, Russia
 - 49: Also at Albert Einstein Center for Fundamental Physics, Bern, Switzerland
 - 50: Also at Gaziosmanpasa University, Tokat, Turkey
 - 51: Also at Mersin University, Mersin, Turkey
 - 52: Also at Cag University, Mersin, Turkey
 - 53: Also at Piri Reis University, Istanbul, Turkey

- 54: Also at Adiyaman University, Adiyaman, Turkey
- 55: Also at Ozyegin University, Istanbul, Turkey
- 56: Also at Izmir Institute of Technology, Izmir, Turkey
- 57: Also at Marmara University, Istanbul, Turkey
- 58: Also at Kafkas University, Kars, Turkey
- 59: Also at Istanbul Bilgi University, Istanbul, Turkey
- 60: Also at Yildiz Technical University, Istanbul, Turkey
- 61: Also at Hacettepe University, Ankara, Turkey
- 62: Also at Rutherford Appleton Laboratory, Didcot, United Kingdom
- 63: Also at School of Physics and Astronomy, University of Southampton, Southampton, United Kingdom
- 64: Also at Instituto de Astrofísica de Canarias, La Laguna, Spain
- 65: Also at Utah Valley University, Orem, USA
- 66: Also at University of Belgrade, Faculty of Physics and Vinca Institute of Nuclear Sciences, Belgrade, Serbia
- 67: Also at Facoltà Ingegneria, Università di Roma, Roma, Italy
- 68: Also at Argonne National Laboratory, Argonne, USA
- 69: Also at Erzincan University, Erzincan, Turkey
- 70: Also at Mimar Sinan University, Istanbul, Istanbul, Turkey
- 71: Also at Texas A&M University at Qatar, Doha, Qatar
- 72: Also at Kyungpook National University, Daegu, Korea